Ocean Oscillations, Blocking High Pressure Systems and Downslope Winds: Explaining The California Drought/Fire Cycle

Roy Clark PhD

Presentation to IEEE Buenaventura Section

11/16/21

Outline

- Time Scales For Climate Change
  - Plate tectonics, Planetary Motion, Solar Insolation, Ocean Oscillations
- The Greenhouse Effect On A Rotating Water Planet
  - Climate Energy Transfer
  - Convective Mass Transport Coupling to Gravity and Rotation
  - Blocking High Pressure Systems And Downslope Winds
  - Ocean Gyres and Ocean Oscillations
- California Rainfall
- Onshore/Offshore Flow In S. California
- Blocking High Pressure Systems
- What About CO_2?
- Future Climate Trends?

The Time Scales For Climate Change

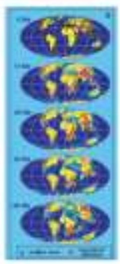

Plate Tectonics

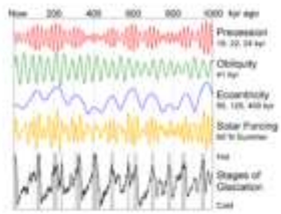

Milankovitch cycles

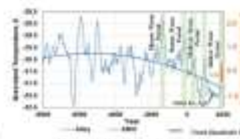

Medieval warming period

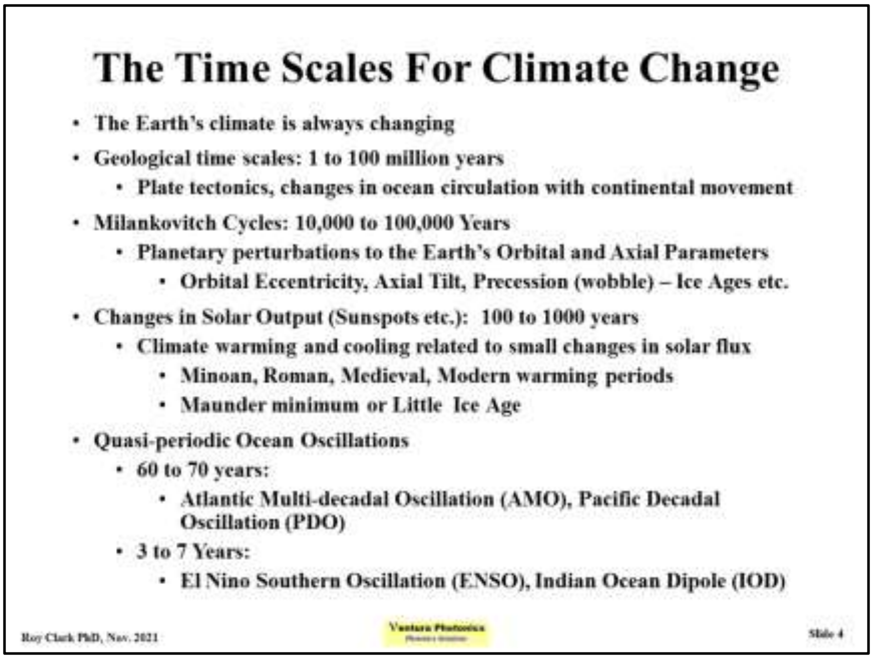

The earth's climate is always changing. Different change mechanisms operate on different time scales.

Over geological time, 1 to 100 million years, climate change is produced by plate tectonics. The ocean circulation changes as the continents move and the ocean boundaries change.

Over the 10,000 to 100,000 year time scale, planetary perturbations, mainly by Jupiter and Saturn alter the orbital eccentricity, axial tilt and precession of the earth. At present the dominant term is the change in eccentricity which cycles the earth through an Ice Age in about 100.000 years.

The sun is a slightly variable star and small changes in solar insolation as measured by sunspot activity and other solar parameters have produced the climate changes known as the Minoan, Roman, Medieval and Modern warming periods and the Maunder minimum or Little Ice Age.

On shorter time scales climate change is caused by quasi-periodic variations in ocean surface temperatures known as ocean oscillations. The Atlantic Multi-decadal Oscillation (AMO) and the Pacific Decadal oscillation (PDO) have periods in the 60 to 70 year range. The PDO also changes on the 15 to 25 year time scale. The El Nino Southern Oscillation (ENSO) and the Indian Ocean Dipole (IOD) are short period oscillations in the 3 to 7 year range.

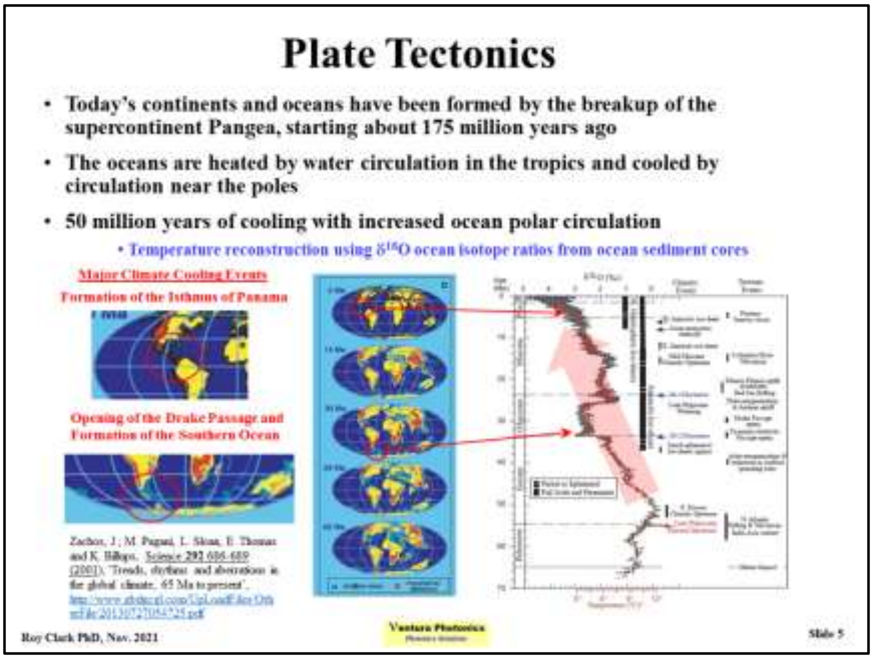

Todays continents and oceans were produced by the breakup of the supercontinent Pangea that started about 175 million years ago. The figure shows the location of the continents at 69, 50, 30 and 14 million years ago and their present location. The related temperature changes are derived from $\delta^{18}O$ isotope ratios measure in deep drilled ocean sediment cores. Overall there has been a cooling trend for the last 50 million years as ocean polar circulation has increased.

Major plate tectonic events include the opening of the Drake passage about 30 million years ago and the formation of the Isthmus of Panama about 5 million years ago. The formation of the Drake Passage established the Southern Ocean circumpolar circulation and produce a major cooling event. The Isthmus of Panama close the ocean connection between the Atlantic and Pacific Oceans.

Other tectonic events include mountain uplift in the Andes and Himalayas and other rearrangements of the continental plates.

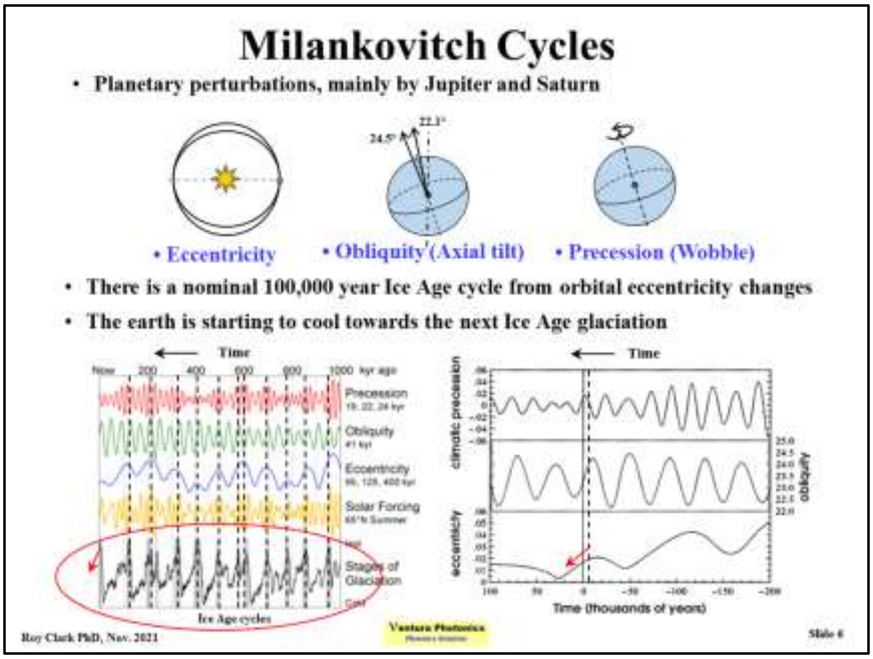

The earth's orbit and axial rotation are perturbed by planetary motions, mainly by Jupiter and Saturn. These perturbations are known as Milankovitch cycles. Changes in the orbital eccentricity change the distance between the sun and the earth. This changes the solar insolation, which is determined by the inverse square law. There are also changes to the axial rotational tilt and the precession or 'wobble' of the rotation axis.

At present, the dominant term is the eccentricity which cycles the earth through an Ice Age on a nominal 100,000 year time scale. The earth reached maximum temperature in the present Ice age cycle about 6000 years ago and is starting to cool.

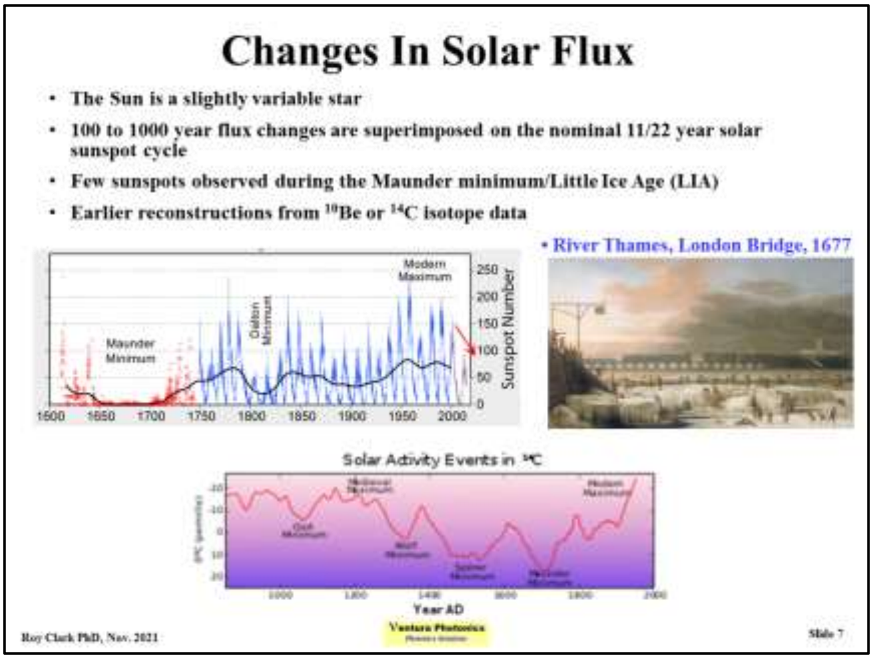

The sun is slightly variable star. There is a nominal 11 year cycle in solar insolation as measured by sunspots and other solar parameters. In addition, there is a magnetic field reversal with each cycle, so a full sunspot cycle is 22 years.

There are also longer term variations in solar output on a 100 to 1000 year time scale. During the Maunder minimum or Little Ice Age (LIA) almost no sunspots were observed and the earth was cooler. The River Thames froze in London so that ice fairs could be held on the river. Since then, the sun has passed through a period of high solar activity known as the modern solar maximum and sunspot activity has decreased over the last two solar cycles. Future solar activity is difficult to predict.

Earlier sunspot activity has been reconstructed using isotope ratios based on ^{10}Be and ^{14}C. This shows a series of maxima including the Minoan, Roman and medieval warming periods.

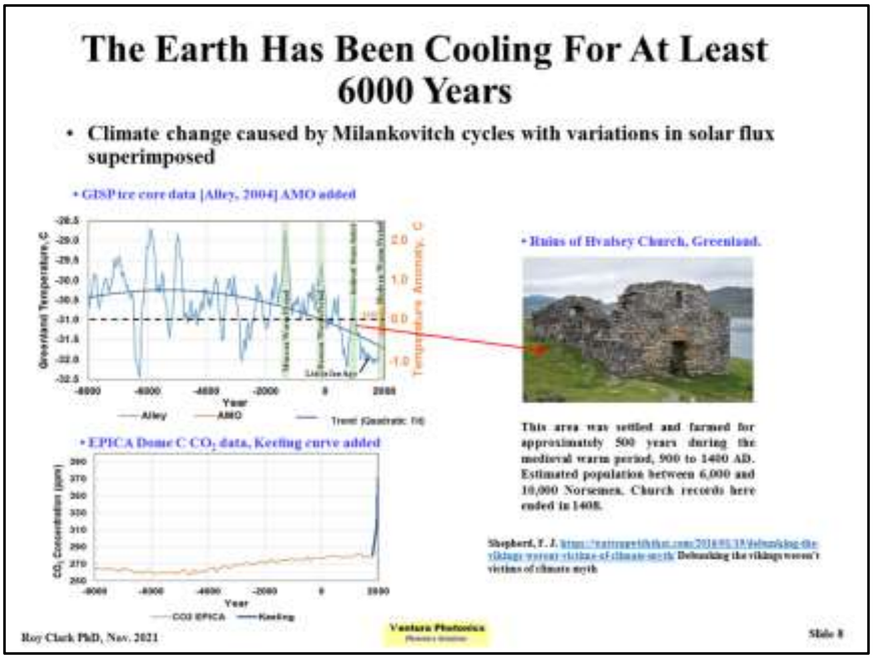

The earth has been cooling for about the last 6000 years. The next Ice Age cooling cycle has started. This cooling has been a ‘roller coaster ride’ with peaks from solar activity superimposed on the downward trend. These solar peaks have had a major impact on human civilization. This trends can be seen in temperature proxy data derived from $\delta^{18}O$ isotope ration analysis of the Greenland GISP deep drilled ice core. The Minoan, Roman, medieval and modern warming periods and the Little Ice Age are indicated. The temperature scale is indicated on the left and the temperature anomaly scale with the mean subtracted is shown on the right. For reference the temperature anomaly of the Atlantic Multi-decadal Oscillation (AMO) is also shown to represent the modern temperature record. This is a separate data set.

Evidence of the medieval warming period can be found in the archaeological record. The picture shows the ruins of Hvalsey Church, Greenland. This area was inhabited by the Norsemen (Vikings) for about 500 years from 900 to 1400 AD. Church records ended in 1408. Peak population has been estimated at between 6000 and 10,000.

The lower plot shows the change in atmospheric CO_2 concentration from the EPICA ice core data. There was little change in CO_2 concentration for 5800 years, so there is no reason to expect that CO_2 suddenly became a major climate drive over the last 200 years.

The Greenhouse Effect On A Rotating Water Planet

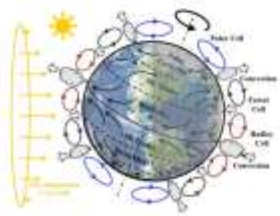

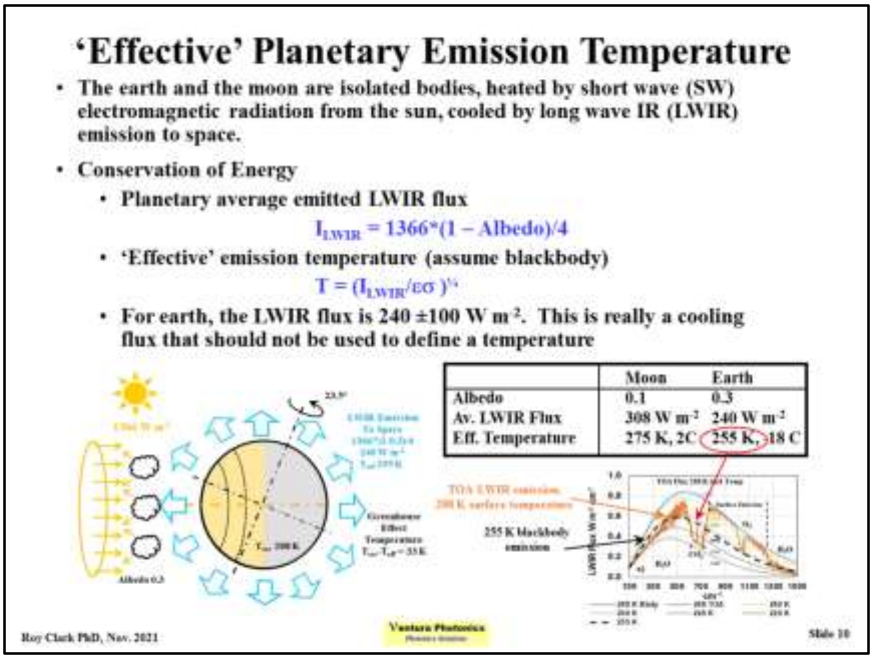

The earth and the moon are isolated bodies that are heated by shortwave (SW) electromagnetic radiation from the sun and cooled by the emission of long wave IR (LWIR) back to space. A ‘planetary average’ LWIR flux may be estimated from a simple conservation of energy argument.

The average solar insolation at the top of the earth’s atmosphere and at the surface of the moon is near 1366 W m^{-2}. The albedo or planetary reflectivities are 0.3 and 0.1. The illumination geometry is that of a circular beam of light incident on a rotating sphere. The area ratio is 4. A simple calculation gives the planetary average flux.

The Stefan-Boltzmann equation may then be used to calculate an ‘effective emission temperature’. This is the surface temperature of an equivalent ‘blackbody sphere’ emitting the average LWIR flux. This is a hypothetical construct that has little useful meaning.

For earth, the planetary average LWIR flux is near 240 W m^{-2}. The local variation with latitude and cloud cover is ±100 W m^{-2}. The effective emission temperature is near 255 K. However, the spectral distribution of the LWIR flux is not that of a blackbody near 255 K. Instead the LWIR flux should be interpreted as a planetary cooling flux. The LWIR radiation is emitted from many different atmospheric levels at different temperatures. . The emission from each level is then modified by the absorption of the levels above.

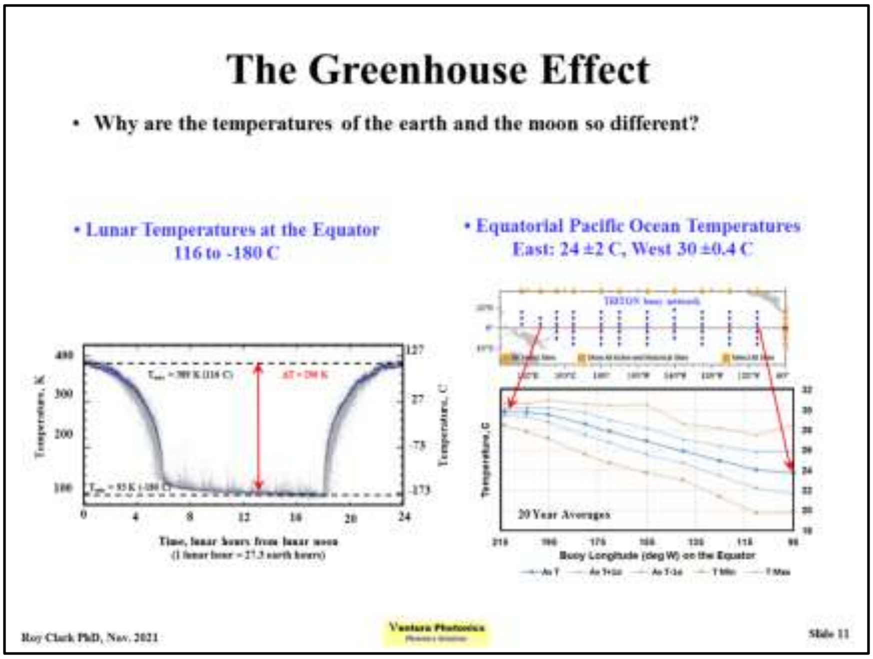

The moon has almost no atmosphere, so the surface is heated by the full intensity of the solar flux during the day and cools by LWIR emission directly to space at night. At the equator, the surface temperature decreases from 116 C at lunar noon to -180 C near the end of the lunar night. A lunar day is almost an earth month, so the surface is approximately in thermal equilibrium with the solar radiation. There is almost no time delay between the change in solar flux and the surface temperature response.

On earth, along the equator in the Pacific Ocean, the long term, 20 year average temperatures are 24 ±2 C in the eastern Pacific and 30 ±0.4C in the western Pacific warm pool.

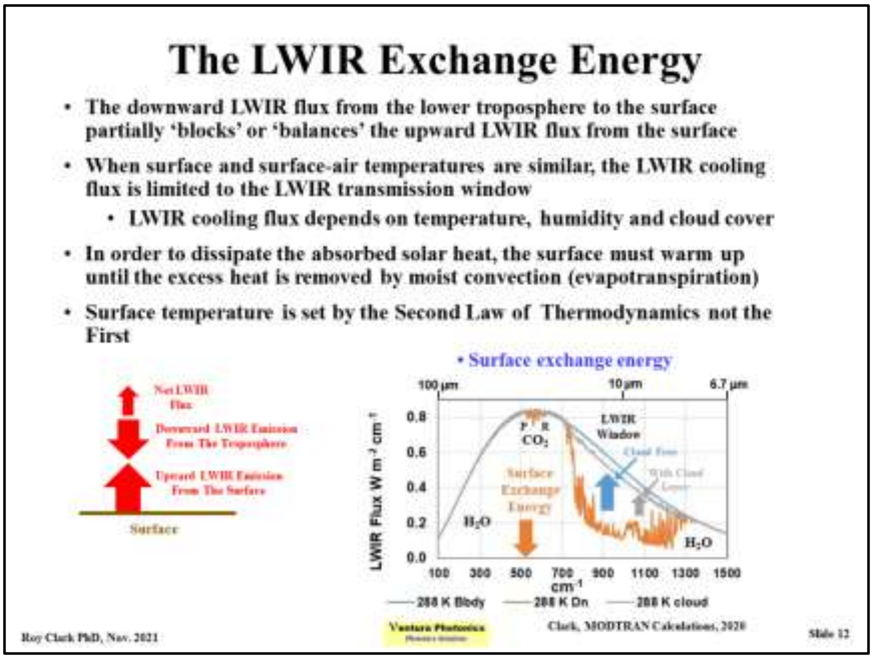

In order to understand the differences in surface temperature between the earth and the moon, it is necessary to consider the interaction of the downward LWIR flux from the lower troposphere with the upward LWIR flux from the surface. When the surface and air temperatures are similar, the downward LWIR flux establishes and exchange energy with the surface. Photons are exchanged, but there is little heat transfer. The surface cooling is limited mainly to net LWIR emission into the atmospheric LWIR transmission window in the 800 to 1200 cm^{-1} spectral region. It involves a cooling flux that does not define a temperature exchange.

Almost all of the downward LWIR flux comes from the first 2 km layer of the troposphere and approximately half comes from the first 100 m layer. This is because of molecular line broadening effects in the lower troposphere.

In order to dissipate the excess absorbed solar flux the surface must warm up until the heat is dissipated by moist convection. The surface temperature is determined by the Second Law of Thermodynamics, not the First. This is real source of the so called greenhouse effect.

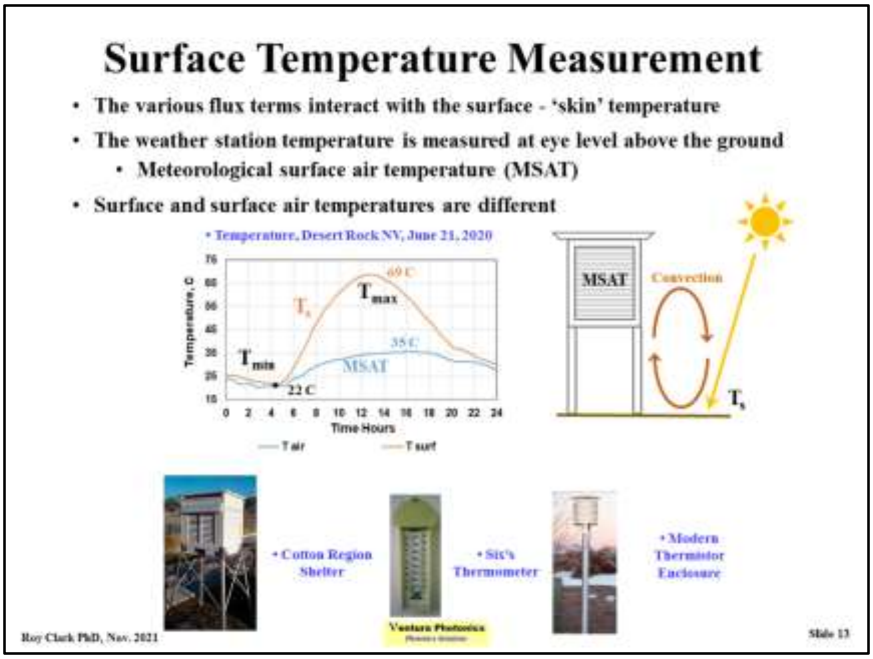

The various flux terms interact with the surface. The temperature at the surface-air interface is sometimes called the skin temperature. However, the weather station temperature is the meteorological surface air temperature which is measured in a ventilated enclosure located at eye level, 1.5 to 2 m above the ground.

In general, the minimum surface and MSAT temperatures are similar. The maximum surface temperature can be significantly higher than the maximum MSAT temperature. This is because the warm air rising from the surface mixes with cooler air at the MAST thermometer level.

Historically, the MSAT was measured in the US using Six's thermometer located in a wooden enclosure known as a cotton region shelter. Starting in the mid 1980s this was replaced by a thermistor located in a smaller 'beehive' enclosure.

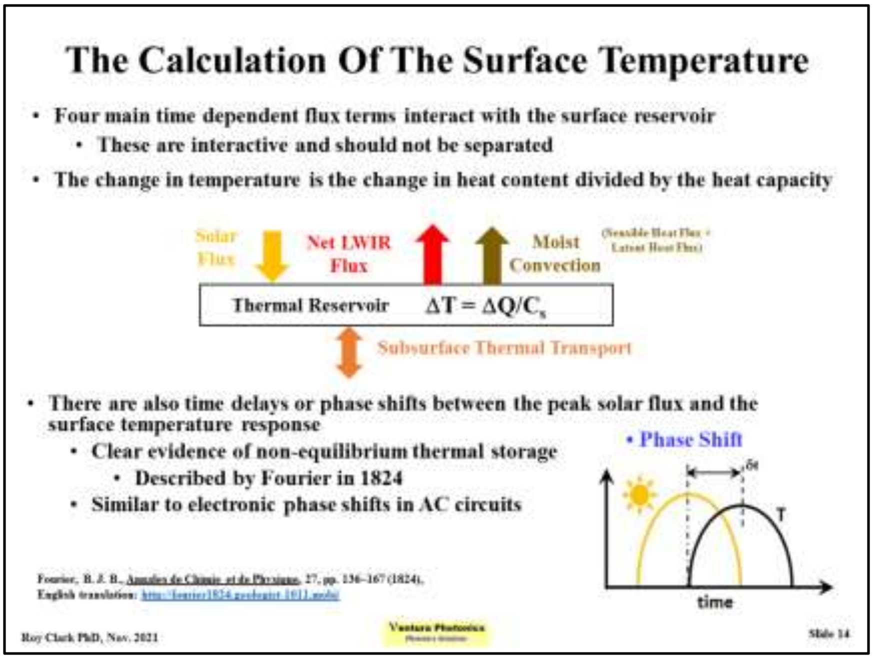

The surface temperature is determined by the change in heat content or enthalpy of the surface thermal reservoir divided by the local heat capacity. There are four main time dependent flux terms that interact with this reservoir. These are the solar flux, the net LWIR cooling flux, the moist convection (evapotranspiration) and the subsurface transport. There are interactive should not be separated and analyzed independently of each other. In particular, a change in LWIR flux cannot be isolated and used with the Stefan-Boltzmann law to calculate a change in surface temperature.

An important part of the time dependent temperature response that has been largely ignored for almost 200 years is the time delay or phase shift between the peak solar flux and the surface temperature response. This was described by Fourier in 1824/1827. There is a diurnal phase shift that may reach 2 or more house. However, this is not normally measured as part of the weather station temperature. There is also a seasonal phase shift of 4 to 8 weeks at mid latitudes. N. hemisphere peak summer temperatures typically occur in August, after the summer solstice near the end of June. This has been recorded as part of the weather station data for well over 100 years.

This phase shift comes from delays in ocean heating carried over land by the prevailing weather systems. The heat capacity of the land thermal reservoir is too small to produce these phase shifts.

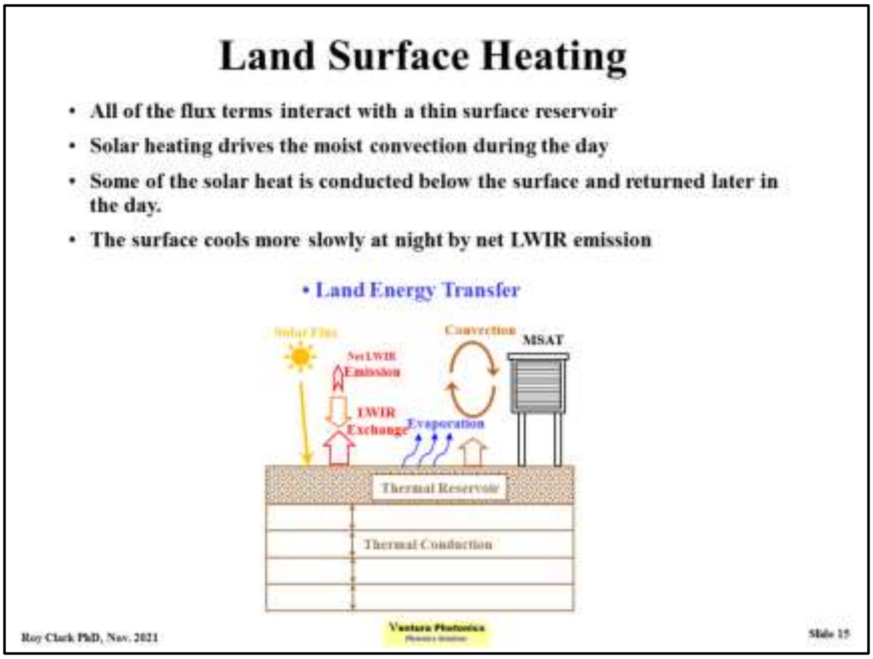

Over land, the surface heating is localized and the subsurface heat transfer is produced by thermal conduction.

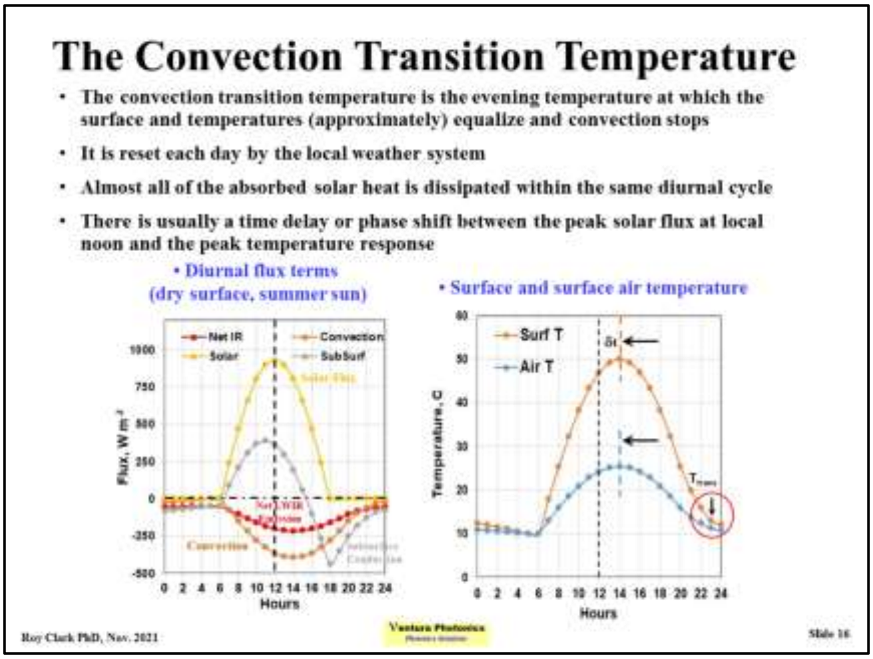

The ground is heated by the sun during the day. As the temperature rises, the surface warms up faster than the air layer above. A thermal gradient is established both between the air above and the subsurface layers below. The surface-air gradient drives the convection and the subsurface gradient conducts heat below the surface. Later in the day as the surface cools, the subsurface thermal gradient reverses and the stored heat is returned to the surface. Convection slows and stops as the land and air temperatures equalize in the evening. This convection transition temperature is reset each day by the local weather system passing through.

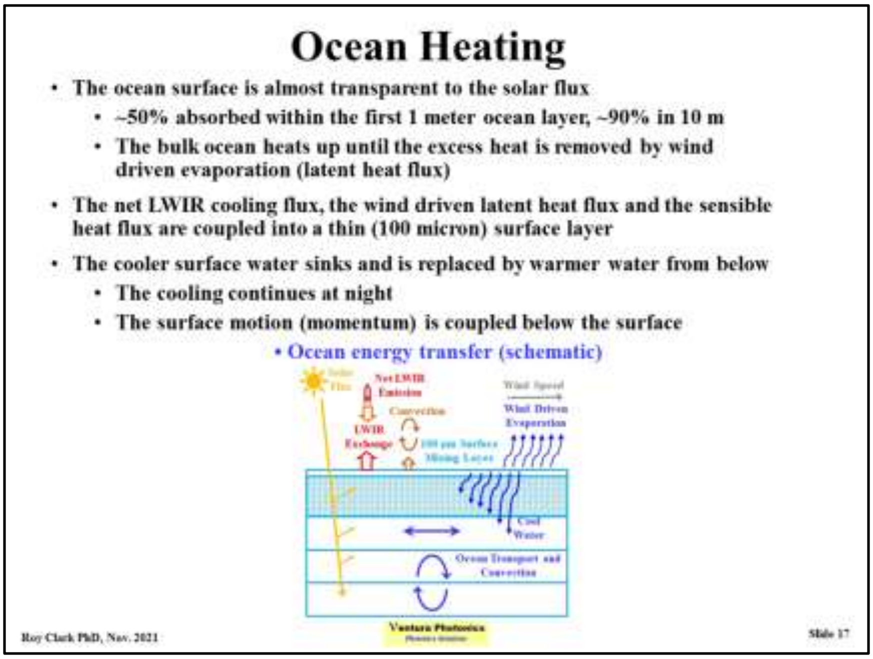

The ocean surface is almost transparent to the solar flux. Approximately half of the solar flux is absorbed within the first 1 meter layer of the ocean and 90% is absorbed within the 10 m layer. In order to dissipate the absorbed solar heat, the bulk ocean temperature increases until the heat is removed by wind driven evaporation or latent heat flux.

The penetration depth of the LWIR flux into the ocean surface is less than 100 micron

Ocean Temperatures

- Diurnal temperature rise is small, decreases with increasing wind speed
  - Evaporation or latent heat flux increases with wind speed
- Heat is stored in the ocean by summer heating and released in winter
- Significant phase shifts indicant non-equilibrium thermal transfer

• TRITON Buoy data
July 2010, 165° E, 0° N

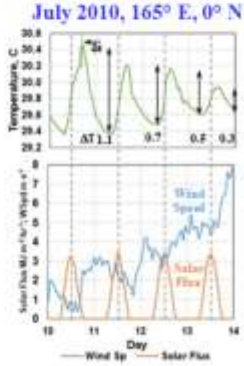

• N. Atlantic Ocean, 20° W, 30° N (Argo data)
west of Canary Islands

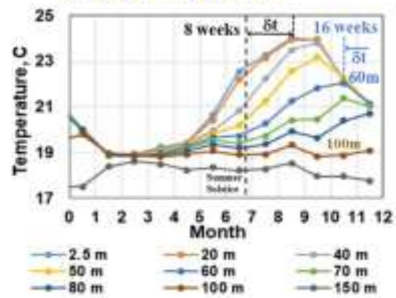

Roy Clark PhD, Nov. 2021

Ventura Photonics

Slide 18

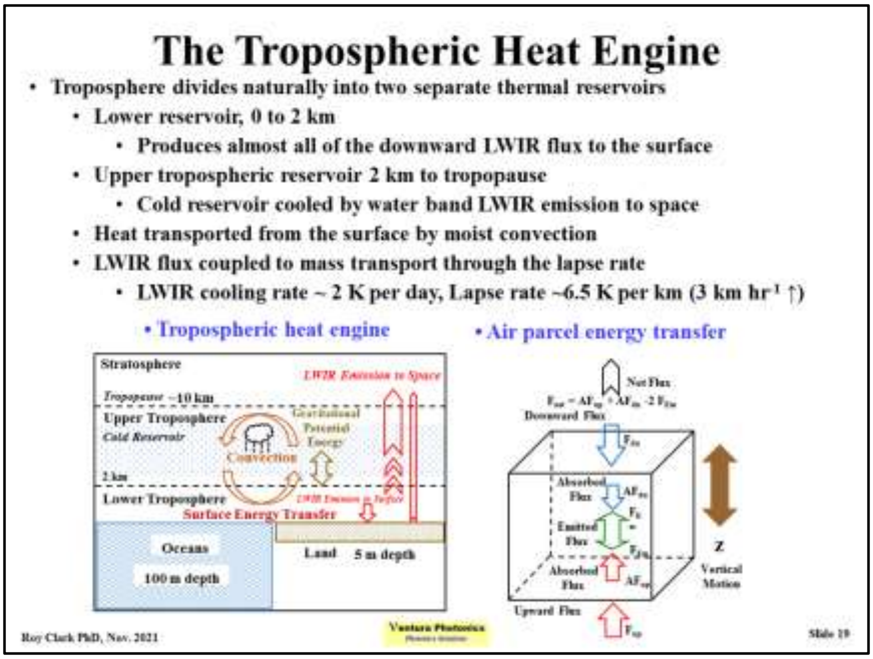

The troposphere functions as an open cycle heat engine that removes part of the surface heat as moist convection. An air parcel in the troposphere absorbs some of the net LWIR flux from the air layers above and below. It also emits LWIR flux at the local air temperature. As the air parcel rises through the troposphere it expands and cools. A typical moist lapse rate is -6.5 K km^{-1}. Because of molecular line broadening effects, almost all of the downward LWIR flux from the troposphere to the surface is emitted from within the first 2 km layer. Approximately half of this flux originates from within the first 100 m layer above the surface. This means that the troposphere splits naturally into two independent thermal reservoirs. The lower tropospheric reservoir extends to 2 km and the upper tropospheric reservoir extends from 2 km to the tropopause. The upper reservoir acts as the cold reservoir of the heat engine. Heat is stored as gravitational potential energy and radiated to space, mainly by LWIR emission from the water bands. This emission is a rate limited process. The rate of emission depends mainly on the local temperature that determines the water vapor pressure. The emission band shifts to higher altitude as the surface temperature increases. The LWIR flux and the mass transport are coupled and should not be analyzed independently of each other. The tropospheric heat engine and the energy transfer processes for a local air parcel are shown.

Convection, Rotation and Gravity

- **Convection is a mass transport process**
- **A rising air parcel in the troposphere is coupled to the earth's gravitational field and rotation (angular momentum)**
  - **The air expands and cools as it rises**
    - **The tropospheric temperature decrease with altitude (lapse rate)**
    - **Water vapor condenses above the saturation level (clouds and rain)**
    - **Latent heat is released, lapse rate is reduced**
    - **Internal molecular energy is converted to gravitational potential energy**
    - **Heat is radiated back to space, mainly by the water bands**
  - **The moment of inertia increases and the angular velocity decreases**
    - **This produces the trade winds**

• Convective coupling

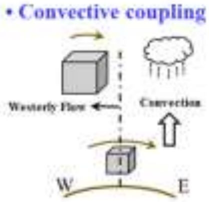

• Tropospheric Lapse Rate

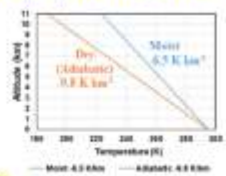

The Earth's Convective Cell Structure

- Convection produces the Hadley, Ferrell, Polar cell structure
- Downward flow of dry air produces desert conditions near 30° latitudes
- Convective flow is coupled to the earth's rotation (Coriolis effect) to give the Mid latitude cyclone/anticyclone structure
- Trade winds drive the ocean gyre circulation

• Convective cell structure and trade winds

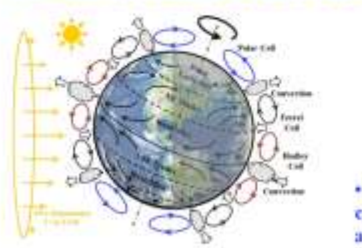

• Convective cell structure and jet streams

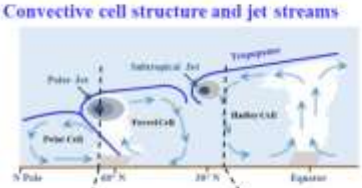

• Mid latitude cyclones and anticyclones

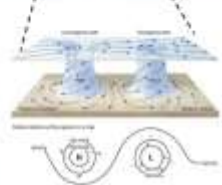

Blocking High Pressure Systems

- As dry air descends, the warming rate is 9.8 C per kilometer
  - The heat source is air compression
- Heat accumulates in a stationary blocking high pressure system
- Other weather systems move around the blocking high

• High pressure dome over the Pacific NW, June 27 th 2021

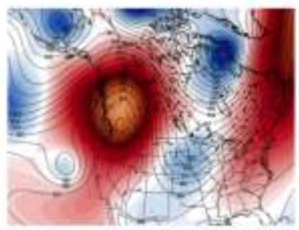

• Overnight temperature drop in Portland OR June 28 to 29 was 52 F from 116 to 64 F (29 C from 47 to 18 C)

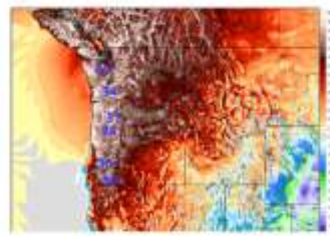

Downslope Winds

- Santa Ana Winds, (S. CA) Diablo Winds (N. CA), Chinook Winds (Rockies), Föen winds (Alps)
- Dry air compressed by downslope flow
  - Can be associated with a blocking high pressure system
  - Rapid changes in temperature

• Thomas fire, Ventura, 12/5/17
Terra Satellite Image

• Chinook Event
Havre, Montana, Dec 16 to 18, 1933

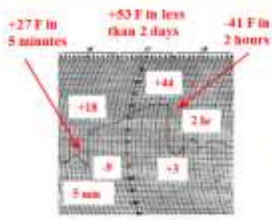

•Thermograph Trace

• Santa Ana Winds

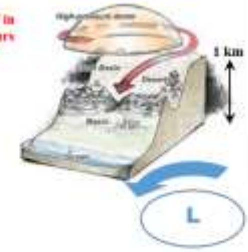

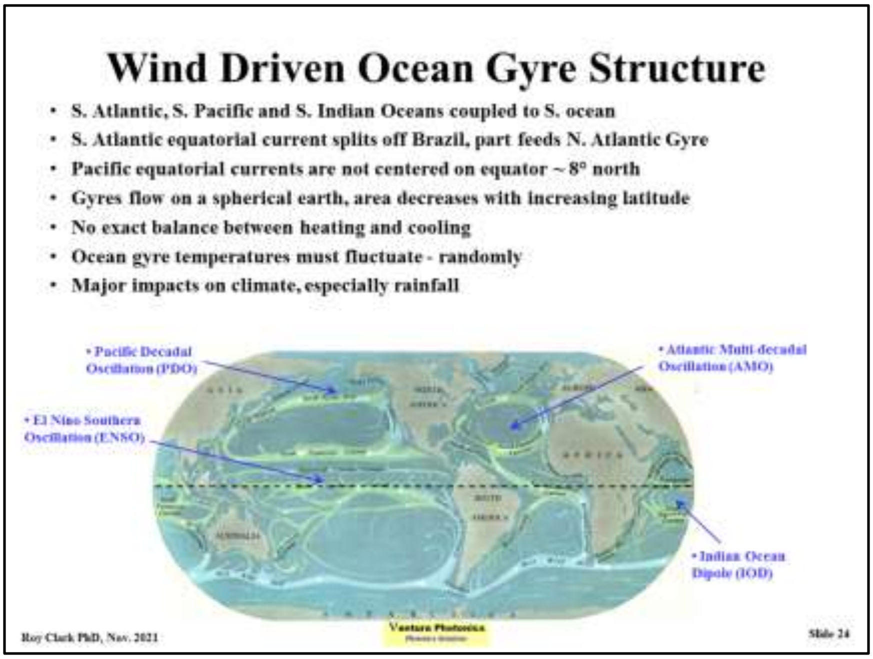

The trade winds drive the ocean gyre structure. There are 5 main ocean gyres in the N. and S. Pacific Ocean, the N. and S. Atlantic Ocean and the S. Indian Ocean. The three southern gyres are coupled to the Southern Ocean circulation. The center of the gyre flow is about 8° N. of the equator. Part of the S. Atlantic equatorial current is diverted northwards off the coast of Brazil. The gyres are circulating on a sphere. The area decreases with latitude which drives the gyre currents to lower depths at higher latitudes.

There is no requirement for an exact flux balance between the solar heating and the surface cooling within the ocean gyre circulation. Natural variation in the heating and cooling produces characteristic quasi-periodic ocean temperature oscillations. There are four principal ocean oscillations. The El Nino Southern Oscillation (ENSO) and the Indian Ocean Dipole (IOD) have periods between 3 and 7 years. The Pacific Decadal Oscillation (PDO) has periods between 15 and 25 years and between 50 and 70 years. The Atlantic Multi-decadal Oscillation (AMO) has a period in the 60 to 70 year range. Although the temperature changes may be small, these oscillations have a major impact on the earth's climate because of their effect on rainfall.

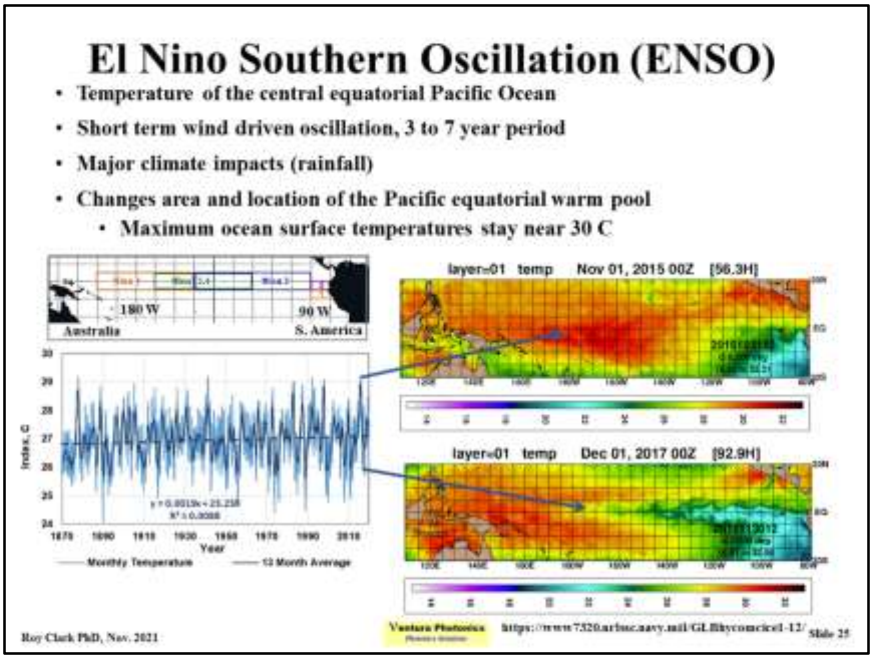

The El Nino Southern Oscillation (ENSO) is the variation in ocean surface temperature in the central equatorial Pacific Ocean. Normally the ENSO 3.5 index is used. This is the area from 120° to 170° W in longitude and ±5° in latitude. The ENSO is a short term oscillation with a period between 3 and 7 years. The maximum ocean temperature stays near 30 C. It is location and extent of the warm pool that changes. The main influence of the ENSO is through changes in rainfall patterns.

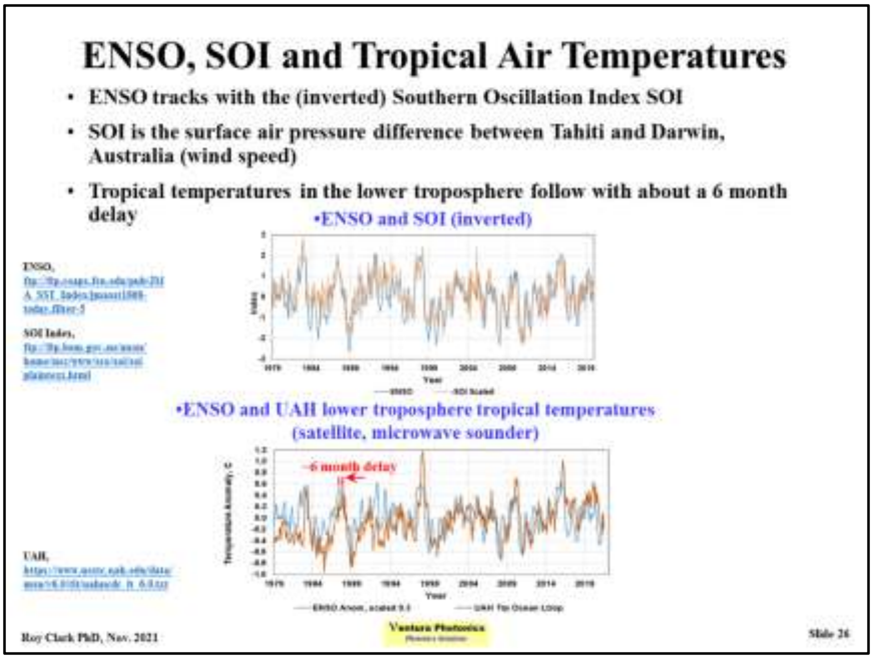

The ENSO is a wind driven oscillation. This may be seen by comparing it to the Southern Oscillation Index (SOI). The SOI is the surface air pressure difference between Tahiti and Darwin Australia. A higher index means a higher wind speed and a lower surface temperature so there is an inverse relationship between the SIO and the ENSO. This is shown in the upper plot.

The ENSO surface temperature changes couple into the troposphere and the lower troposphere tropical temperature follows within about 6 months. This is shown in the lower plot.

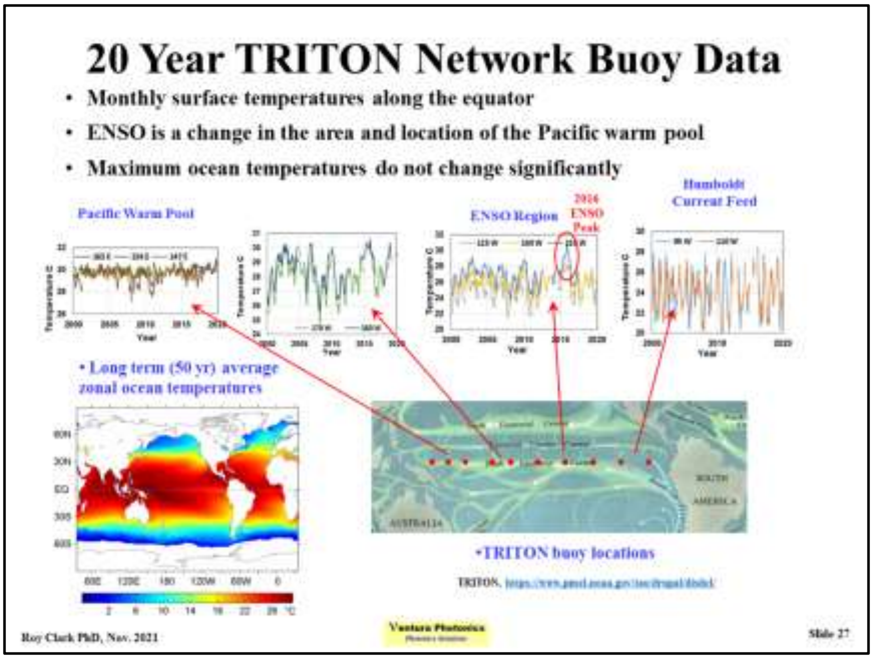

The ENSO is part of the equatorial gyre circulation. Cooler water is fed into the S. Pacific equatorial current from the Humboldt current. The average temperature is near 24 C and the fluctuations are the seasonal variations in temperature in the S. Pacific gyre. The temperatures increase and the magnitude of the fluctuations decrease as the water flows westwards leading to the formation of the equatorial Pacific warm pool in the W. Pacific Ocean. The figure shows the available monthly temperature data for the 20 year period from 2000 to 2019. Blocks of data may be missing because of sensor failure.

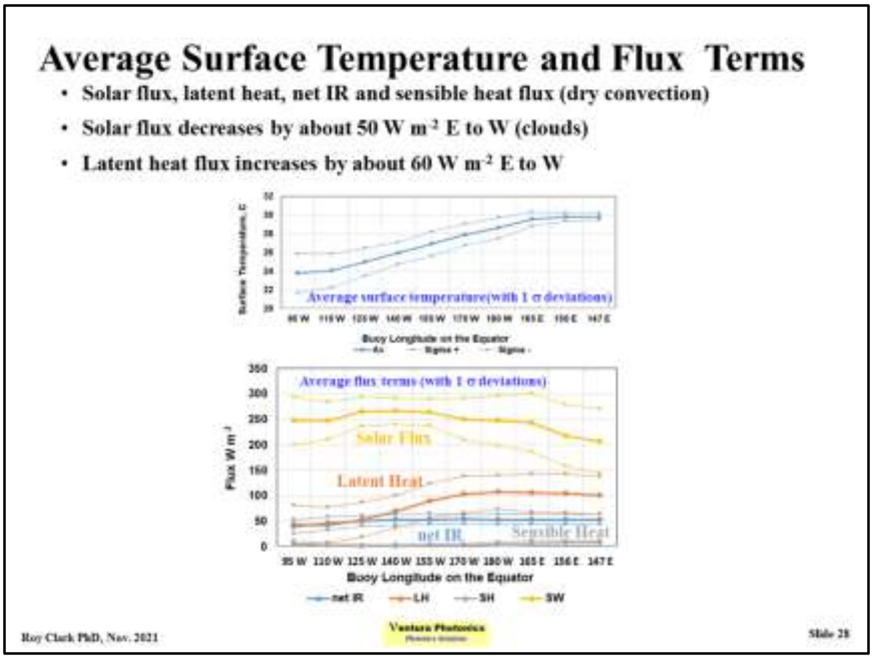

The surface temperature in the equatorial Pacific ocean increases from 24 C at 95° W to 30 C in the western warm pool. The average daily solar flux decreases from approximately 250 W m^{-2} to 200 W m^{-2} as the cloud cover increases. The latent heat flux increases from approximately 40 to 100 W m^{-2}. The net LWIR cooling flux only increases by about 10 W m^{-2} from 40 to 50 W m^{-2}. The sensible heat flux remains small, below 10 W m^{-2}.

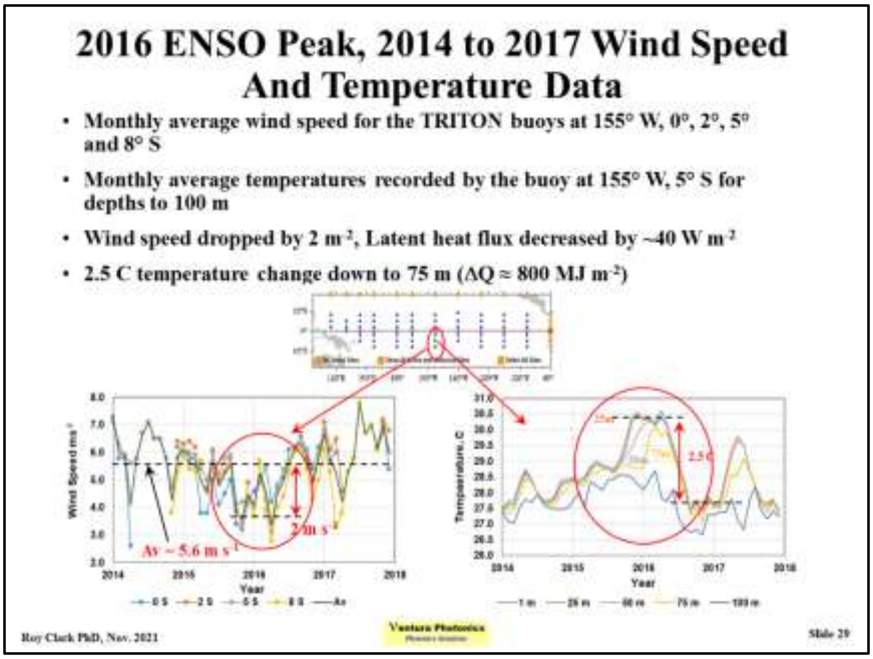

During the 2016 ENSO peak, the average monthly wind speed measured by the TRITON buoys at 155° W, 0°, 2°, 5° and 8° S decreased by approximately 2 m s^{-1} from the 4 year, 2014 to 2017 average of 5.6 m s^{-1}. The decrease in latent heat flux was approximately 40 W m^{-2}. This produced an increase in ocean temperature of 2.5 C down to a depth of 75 m. When the wind speed increased a few months later, the temperature decreased by 2.5 C down to 75 m. The corresponding change in ocean heat content was approximately 800 MJ m^{-2}.

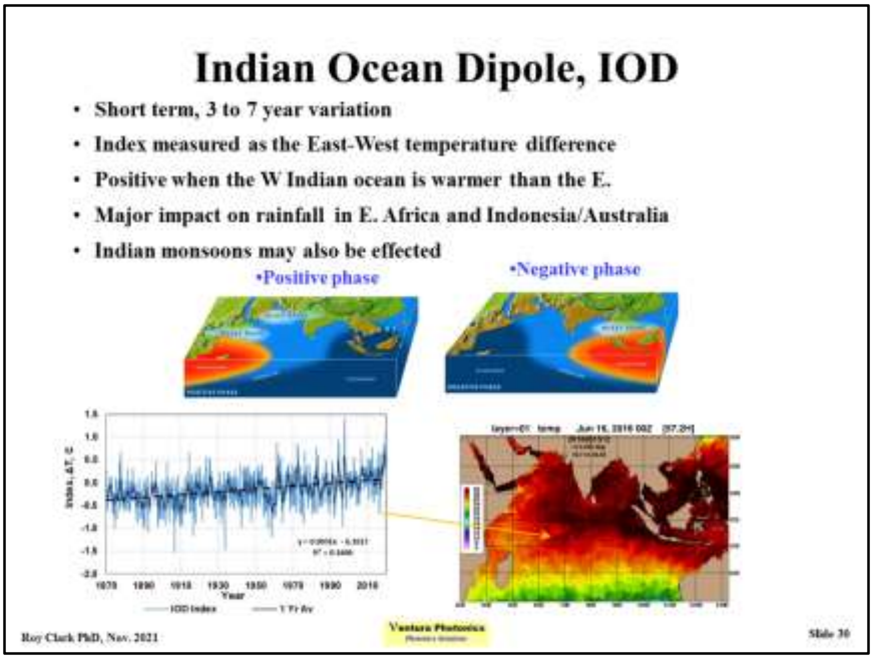

The Indian Ocean Dipole (IOD) is the difference in temperature between the western and eastern regions of the Indian Ocean. This is a short period, 3 to 7 year oscillation. A positive index indicates a higher temperature and higher rainfall over the western Indian Ocean near Madagascar and the E. African coast. A negative index indicates higher temperatures and rainfall over the eastern Indian Ocean near Indonesia and parts of Australia.

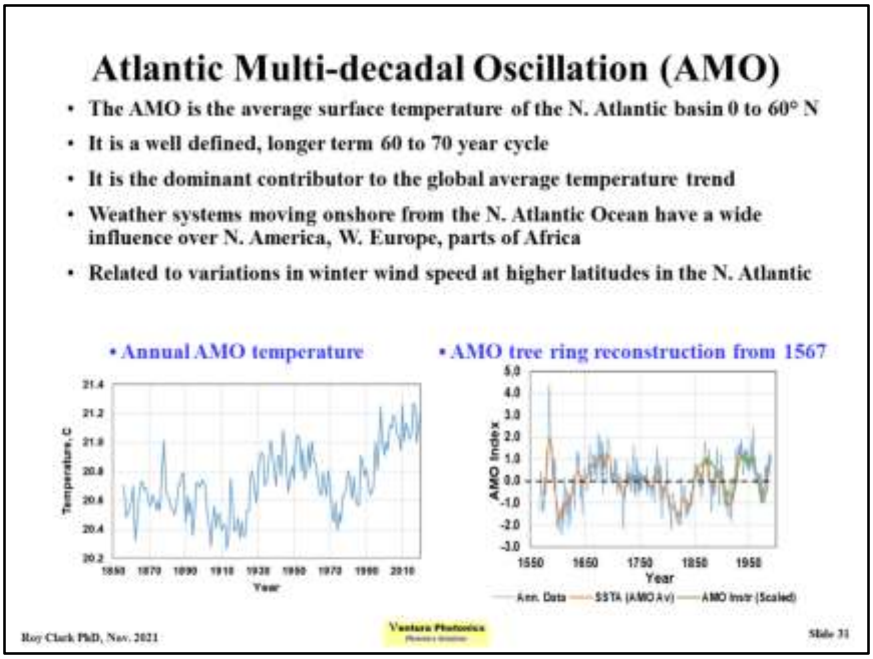

The Atlantic Multi-decadal Oscillation (AMO) is the change in the surface temperature of the N. Atlantic basin from 0° to 60° N. It is a well defined long term oscillation with a period between 60 and 70 years.

It is the dominant contributor to the global average temperature trend in such series as HadCRUT4. The IOD and PDO are dipoles or temperature differences that tend to cancel in the global average. The ENSO involves a relatively small temperature change, but with a large impact on rainfall. The influence of the AMO extends over larger areas of N. America, W. Europe and parts of Africa as weather systems move onshore from the N. Atlantic Basin.

The AMO is related to changes in winter wind speed at higher latitudes in the N. Atlantic Ocean.

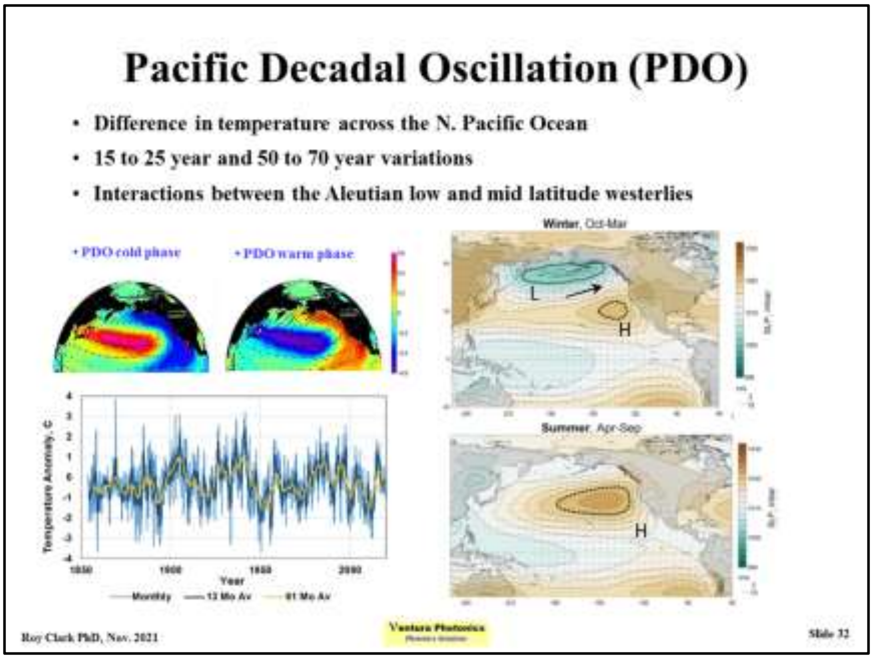

The Pacific Decadal Oscillation (PDO) is a medium to long term, 15 to 25 and 50 to 70 period variation in the temperature difference across the N. Pacific Ocean. It is associated with changes in winter wind speed related to the Aleutian low and mid latitude westerlies.

The warm phase of the PDO is associated with higher rainfall along the W. coast of N. America.

California Rainfall

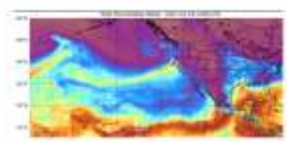

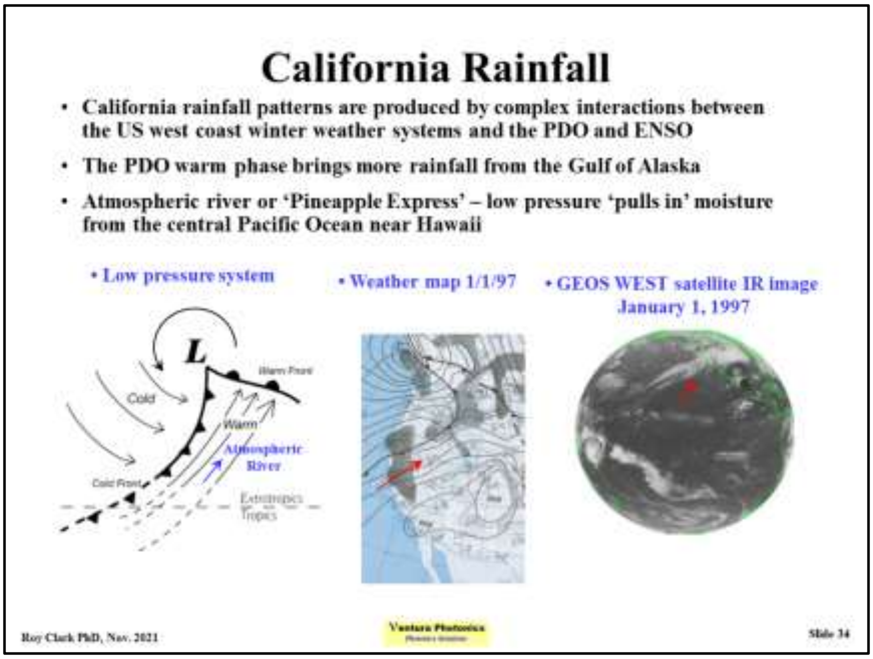

California rainfall is determined by complex interactions between the US west coast weather systems and the PDO and ENSO.

The warm phase of the PDO brings more rain to California.

As the low pressure systems move down the coast they can 'pull in' warm air from the mid Pacific Ocean. This creates 'atmospheric rivers' or a 'Pineapple Express' with moisture originating from regions near Hawaii.

The map and image show the weather map for January 1, 1997 and the GEOS West satellite IR image. The low pressure system has established an 'atmospheric river' that is pulling in moisture from the central N. Pacific Ocean.

The creation of an atmospheric river depends on the extent of the low pressure region, the phase of the PDO and the state of the ENSO in the equatorial Pacific Ocean.

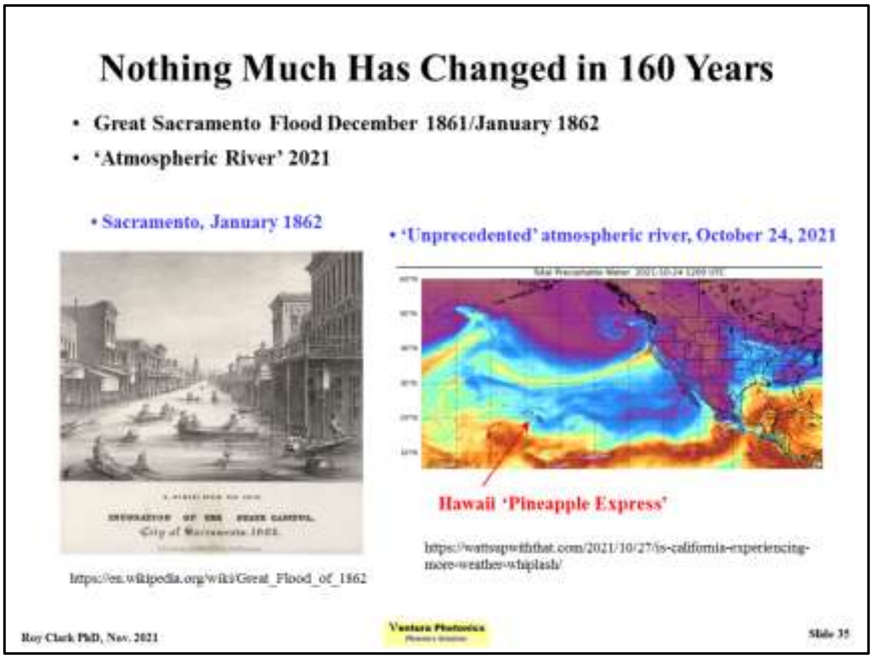

Nothing much has change in 160 years. Sacramento was flooded in December 1861/January 1862 by two successive 'atmospheric rivers'. We have just an 'atmospheric river' produce rainfall over N. California.

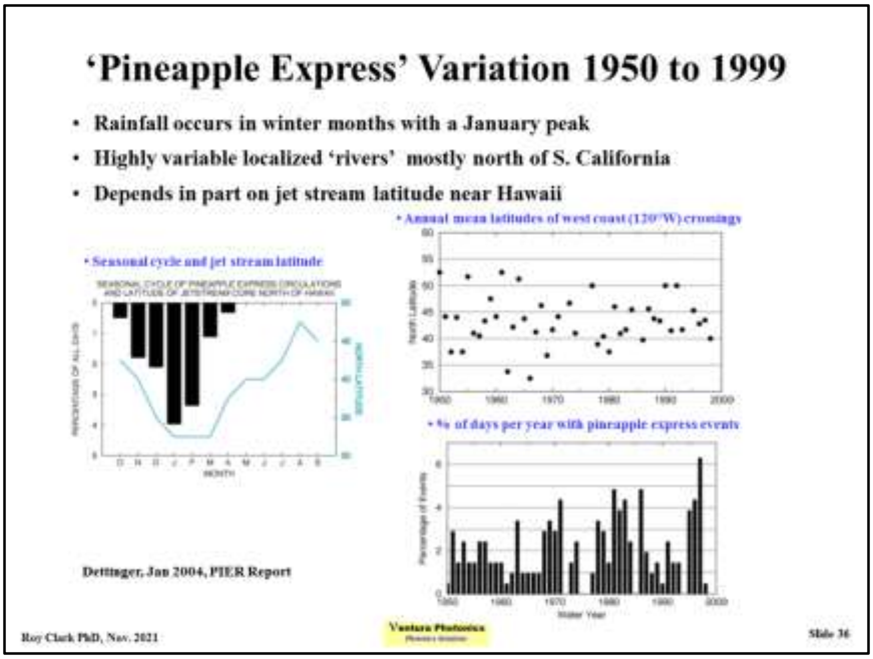

California rainfall is highly variable because of the coupling of the low pressure systems to the moist air in the central Pacific Ocean. The rainfall generally occurs in winter with a peak in January. The atmospheric rivers are relatively narrow bands of rainfall that can cross the N. American coast over a wide range of latitudes. The number of days per year with such rivers is also highly variable.

Onshore/Offshore Flow In S. California: Measurements At Limestone Regional Park, Irvine, 2008

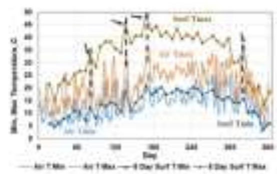

Roy Clark PhD, Nov. 2021

Ventura Photonics

Slide 37

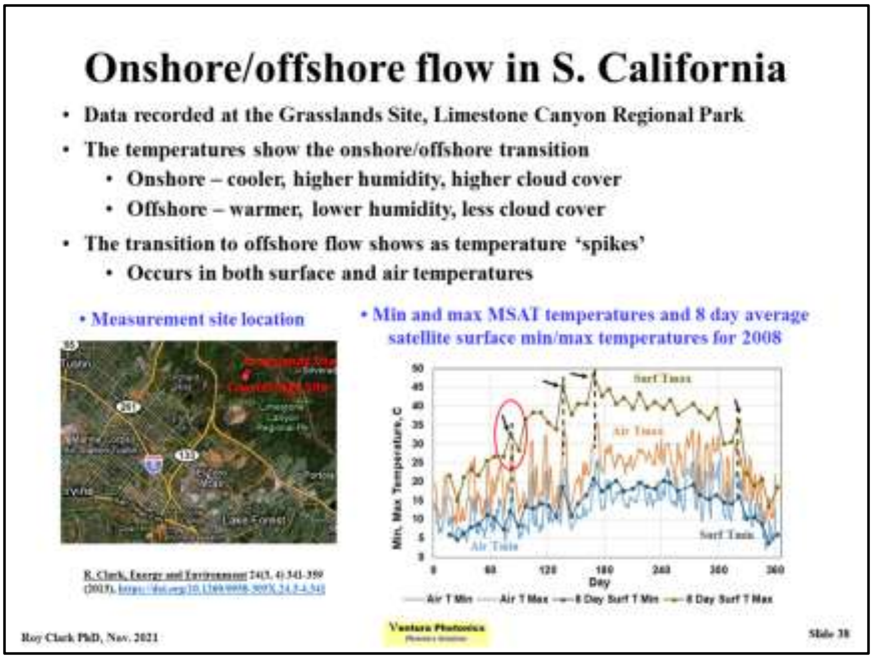

The S. California climate is dominated by two weather patterns. There is an onshore flow produce by low pressure systems near the coast. This produces higher humidity, lower temperatures and increased cloudiness. With a high pressure system over land, the weather pattern reverses to an offshore flow. This produces higher temperatures, lower humidity and reduced cloud cover.

The plot shows the daily maximum and minimum MSAT temperatures recorded during 2008 at an Advanced Radiometric Measurement (ARM) monitoring site located in Limestone Canyon Regional park near Irvine CA. The site was operated by UC Irvine. In addition, 8 day average surface temperatures from satellite data are shown.

There are characteristic spikes in the minimum and maximum temperatures that indicate the onshore/offshore transition. The circled transition near day 80 will be discussed in more detail below. The maximum surface temperature is higher than the maximum MSAT. The temperature difference is approximately 15 C during the summer. The surface temperature also shows the onshore/offshore spikes, although these are reduced by the 8 day averaging.

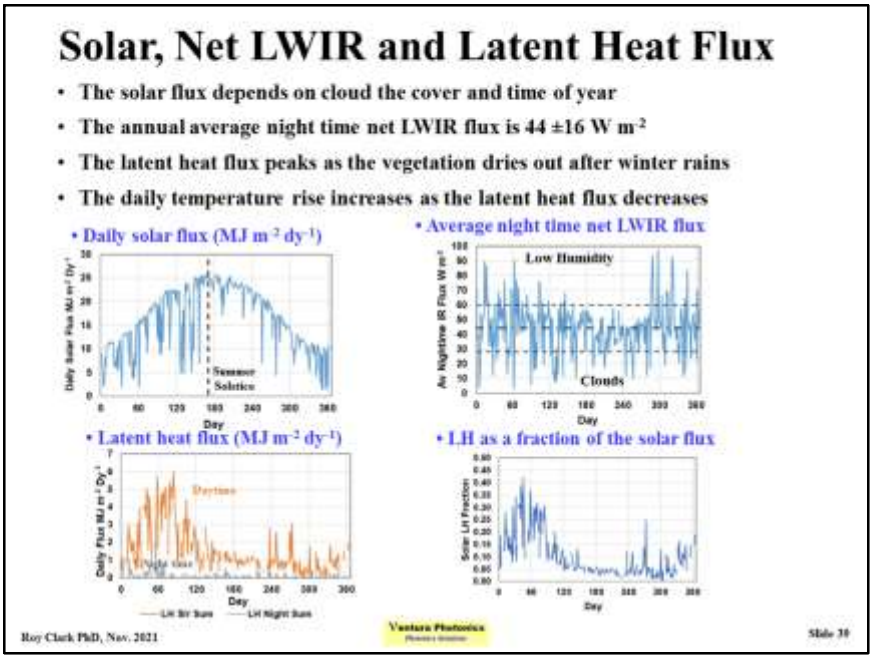

This shows the solar, net LWIR and latent heat fluxes for the 2008 temperature data shown in the previous slide. The solar flux peaks with the summer solstice near the end of June. The decreases in solar flux are produced by clouds mainly related to onshore flow conditions. The average night time net LWIR cooling flux is 44 ±16 W m^{-2}. The magnitude increases with lower humidity during offshore flow and decreases with increasing cloud cover during onshore flow.

The latent heat flux peaks in spring as the vegetation dries out after the winter rains. Up to approximately one third of the solar flux is converted to latent heat during the spring. Later in the year, this solar heat heats the surface during the day.

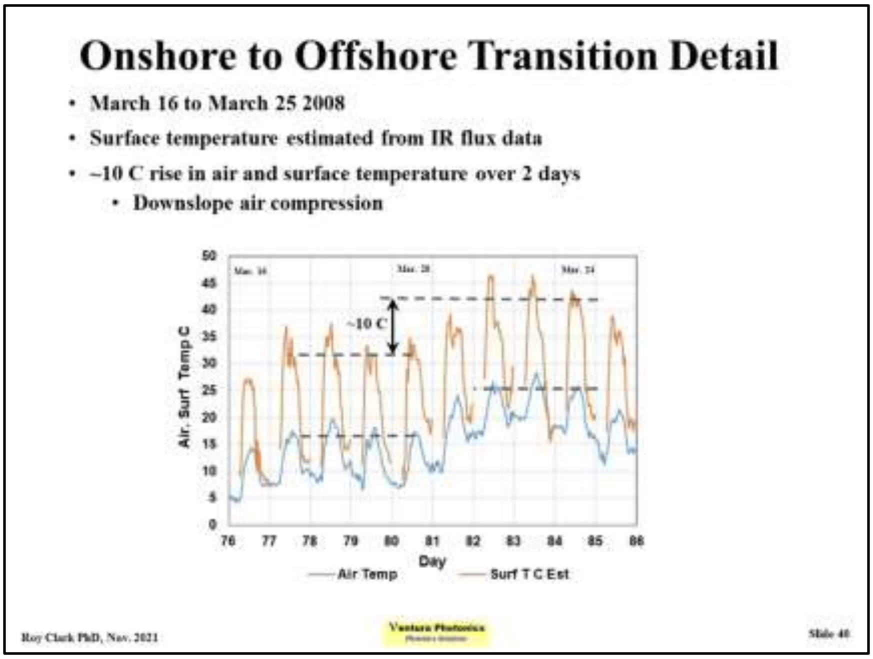

During this onshore to offshore flow transition, the temperature increased by 10 C over 2 days during March 2008. The heating was produced by air compression related to downslope winds from a high pressure system over land. The temperature pattern simply shifted upwards by 10 C. The convective transition temperature also changed by 10 C so that more heat remained stored in the surface thermal reservoir.

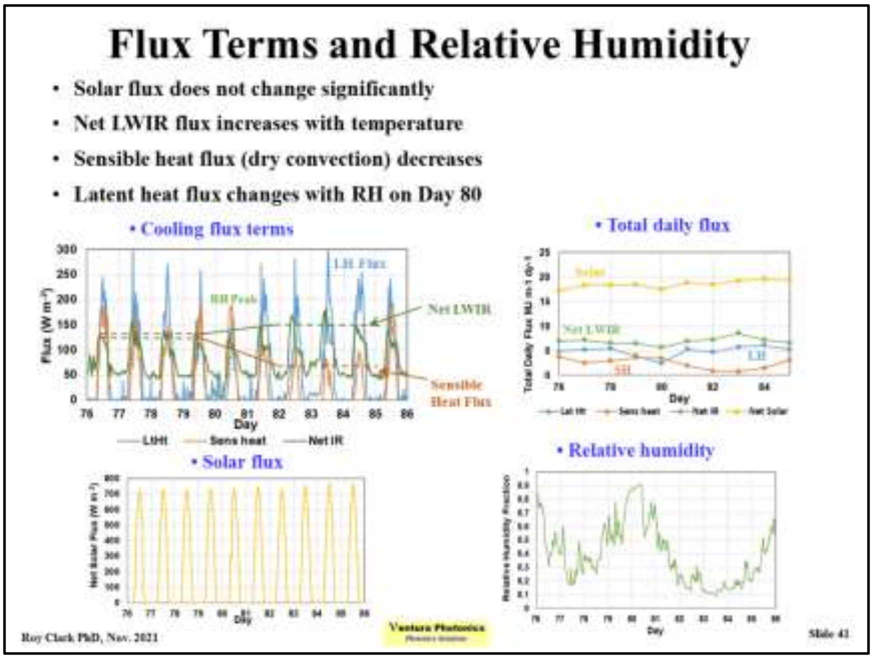

During this onshore/offshore flow transition, the solar flux did not change significantly. There was peak in the relative humidity on day 80 that reduced the latent heat flux. When the air temperature increased, so did the surface temperature so the net LWIR cooling flux increased and the sensible heat flux or dry convection decreased.

Blocking High Pressure Systems, Woomera, Australia

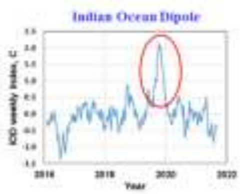

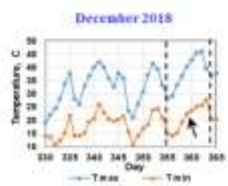

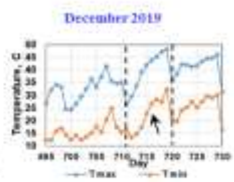

Roy Clark PhD, Nov. 2021

Ventura Photonics

Slide 42

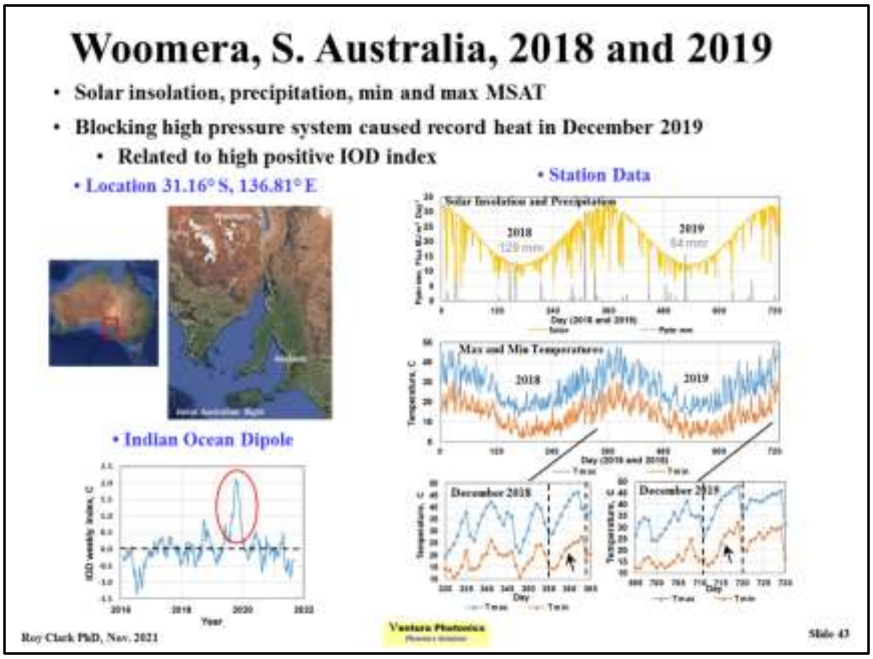

The S. Australia climate is similar to parts of S. California. The dominant weather pattern is a series of high pressure systems that produce warming over a few days and then move on. During December 2019 there was a record high temperature set by a combination of high positive IOD index and a persistent high pressure system.

The warm phase of the IOD produced drought over parts of Australia. 2019 rainfall was 54 mm compared to 129 mm for 2018.

Seasons are reversed in the S. Hemisphere so peak solar insolation is in December.

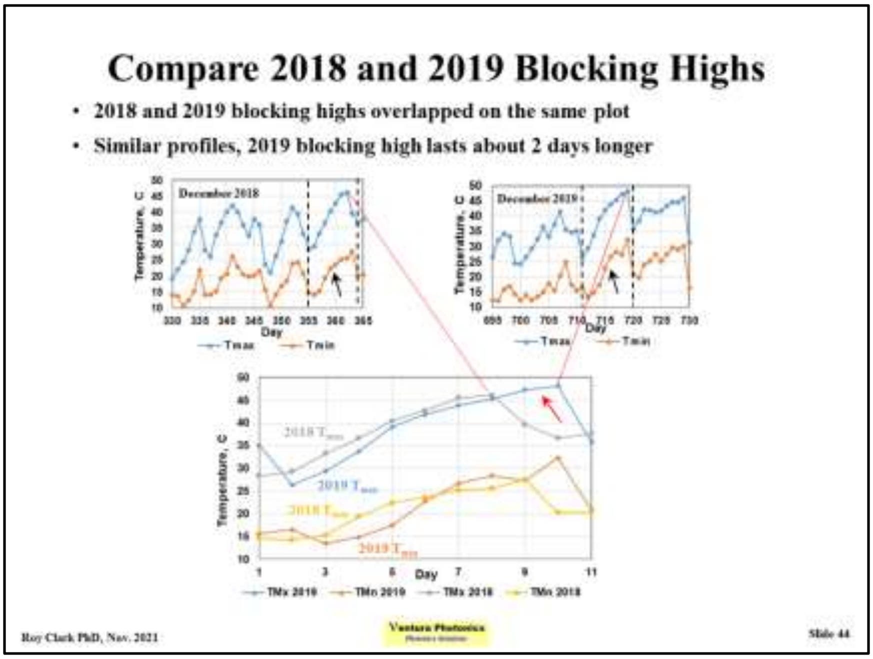

This shows the 2018 and 2019 maximum and minimum temperatures on an enlarged scale. The blocking high pressure events are indicated.

The lower plot shows the 2018 and 2019 high pressure blocking events plotted on the same scale. In 2019, the high pressure system remained over the area for an extra two days causing the record high temperatures.

What About CO_2?

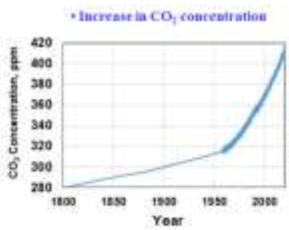

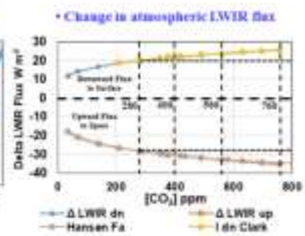

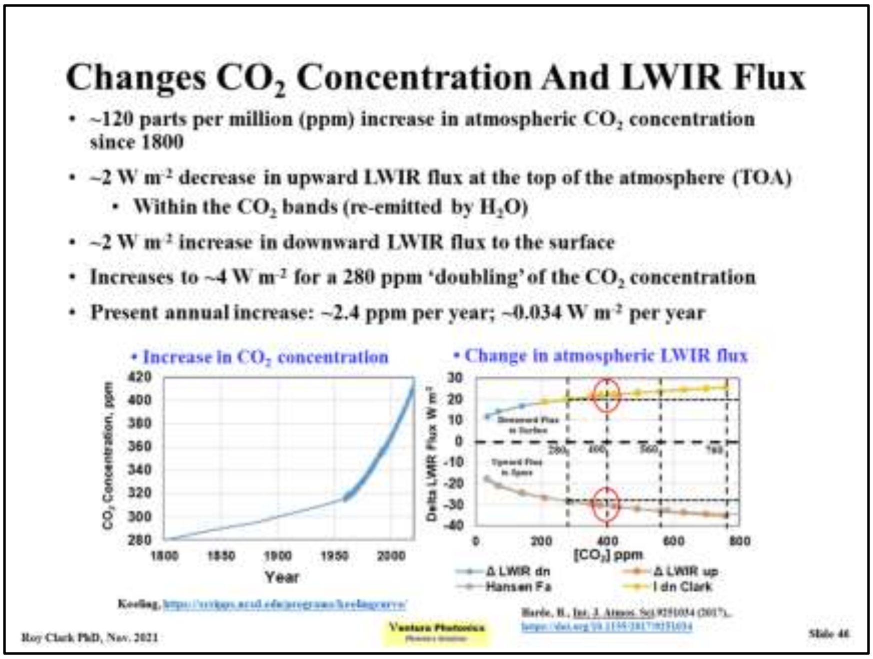

Over the last 200 years, since the start of the industrial revolution, the atmospheric CO_2 concentration has increased by approximately 120 ppm from 280 to 400 ppm (now closer to 420 ppm). It is still increasing.

Radiative transfer calculations show that the increase in CO_2 concentration has produced an decrease in the upward flux at the top of the atmosphere (TOA) of about 2 W m^{-2}. This decrease is caused by atmospheric absorption within the CO_2 bands at lower altitudes. The absorbed heat is then re-emitted as wideband LWIR emission mainly by the water emission bands. It does couple to the surface.

In addition to the reduction in LWIR emission at TOA there is a similar increase near 2 W m_{-2} in the downward LWIR emission to the surface from the CO_2 bands.

Much of the climate modeling discussion focuses on a doubling of the CO_2 concentration from 280 to 560 ppm.

At present, the annual increase in atmospheric CO_2 concentration is near 2.4 ppm per year. The corresponding increase in downward LWIR flux to the surface is near 0.034 W m^{-2}.

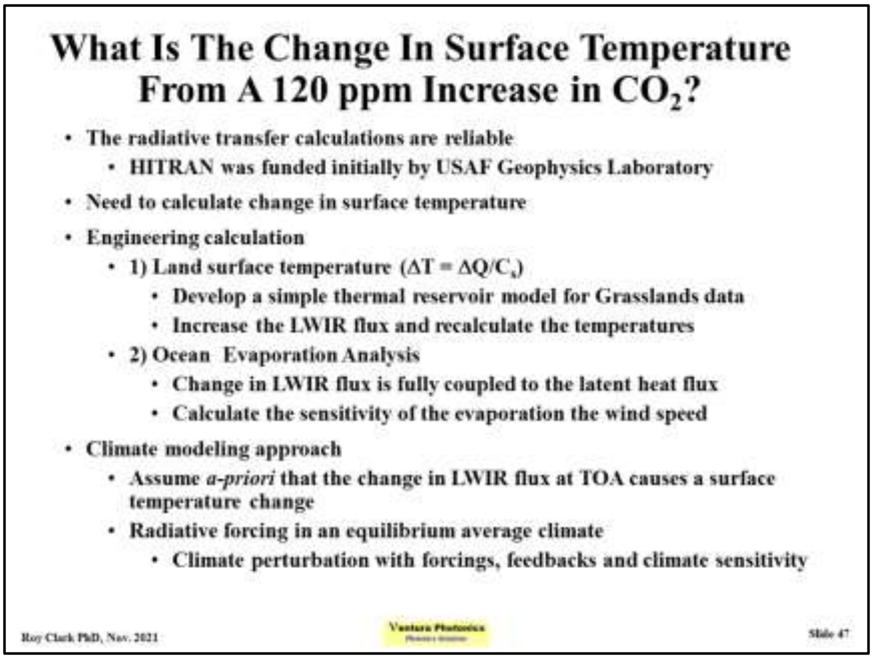

Radiative transfer calculations using the HITRAN database are reliable. HITRAN was initially funded by the USAF Geophysics Laboratory, independent of climate science. The issue is therefore the calculation of the change in surface temperature produced by an increase of 2 W m^{-2} in the downward LWIR flux to the surface. There are two different engineering approaches.

First, the change in temperature of the land thermal reservoir can be calculated using a simple thermal engineering model of the flux terms coupled to the reservoir. The model is configured to match the measured surface temperatures. Then the downward LWIR flux to the surface is increased by 2 W m^{-2} and the model is rerun to determine the temperature increase.

Second, the change in wind speed needed to increase the ocean surface evaporation or latent heat flux by 2 W m^{-2} is determined. This is compared to the normal variation in wind speed driven evaporation.

The climate modeling approach starts from the *a-priori* assumption that the change in LWIR flux, now called a radiative forcing, must cause a change in an 'equilibrium average climate'. It is assumed that the decrease in LWIR flux at TOA produces a perturbation to the 'equilibrium state' and that the surface responds with an increase in temperature to restore the flux balance at TOA. Furthermore, it is also assumed that any change in temperature from CO_2 is amplified by a 'water vapor feedback'. This comes from the fixed RH assumption.

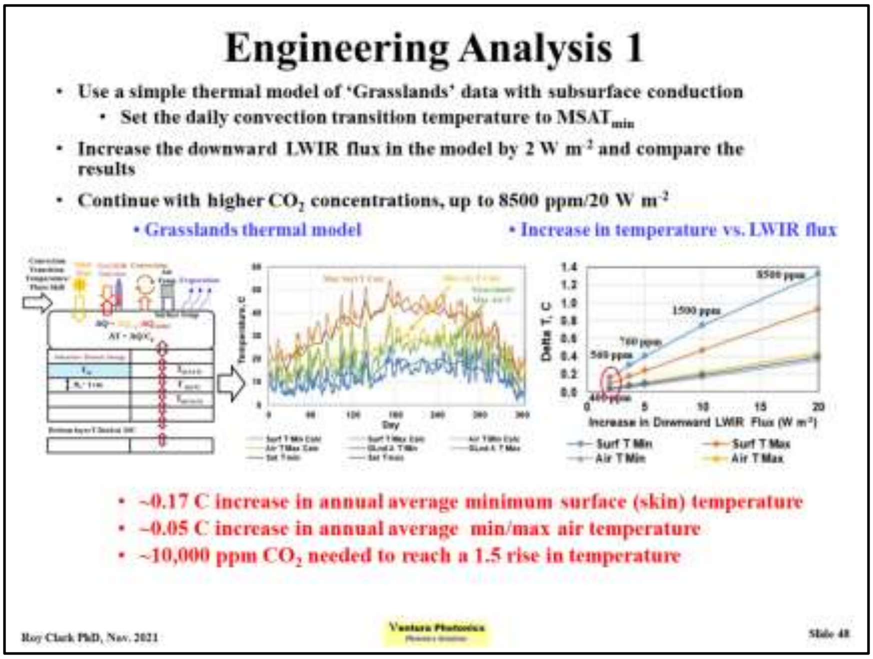

The effect of an increase in CO_2 concentration on the land surface temperature was investigated by building a simple thermal model of the surface energy transfer. The flux terms were coupled to a surface thermal reservoir 1 cm thick. A 2D finite element thermal conduction model was used to simulate the subsurface conduction. The thermal properties of dry sand were used for the model. The minimum MSAT temperatures from the 2008 grasslands data set were used as input for the daily convection transition temperatures. The model was configured to approximately match the output to the measured data. The downward LWIR flux was then increased by 2, 3.7, 5, 10 and 20 W m^{-2} to simulate CO_2 concentrations of 400, 560, 760, 3500 and 8500 ppm.

For an increase of 2 W m^{-2}, the increase in annual average minimum surface temperature was 0.017 C. The increase in MSAT was 0.05 C. When the CO_2 concentration was increased to approximately 8500 W m^{-2} (20 W m^{-2} increase in downward LWIR flux) the average minimum surface temperature increased by 1.3 C. The corresponding MSAT temperatures were near 0.4 C.

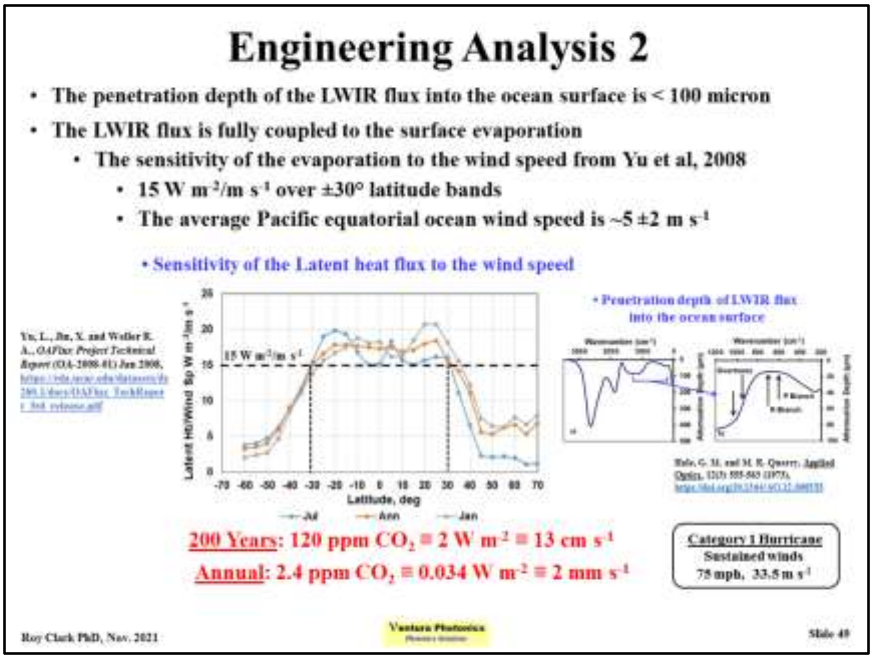

The penetration depth of the LWIR flux into the oceans is less than 100 micron. Here it is fully coupled to the wind driven evaporation or latent heat flux.

Within the ±30° latitude bands, the sensitivity of the latent heat flux to the wind speed is at least 15 W m^{-2}/m s^{-1}.

This means that an increase in wind speed of 13 cm s^{-1} is sufficient to remove all of the heat produced by the 2 W m^{-2} increase in downward LWIR flux from a 120 ppm increase in atmospheric CO_2 concentration.

At present the annual increase in downward LWIR flux to the surface from CO2 is 0.034 W m^{-2}. This is dissipated by a change in wind speed of 2 mm s^{-1}.

For reference, a category 1 hurricane has sustained winds of 75 mph or 33.5 m s^{-1}.

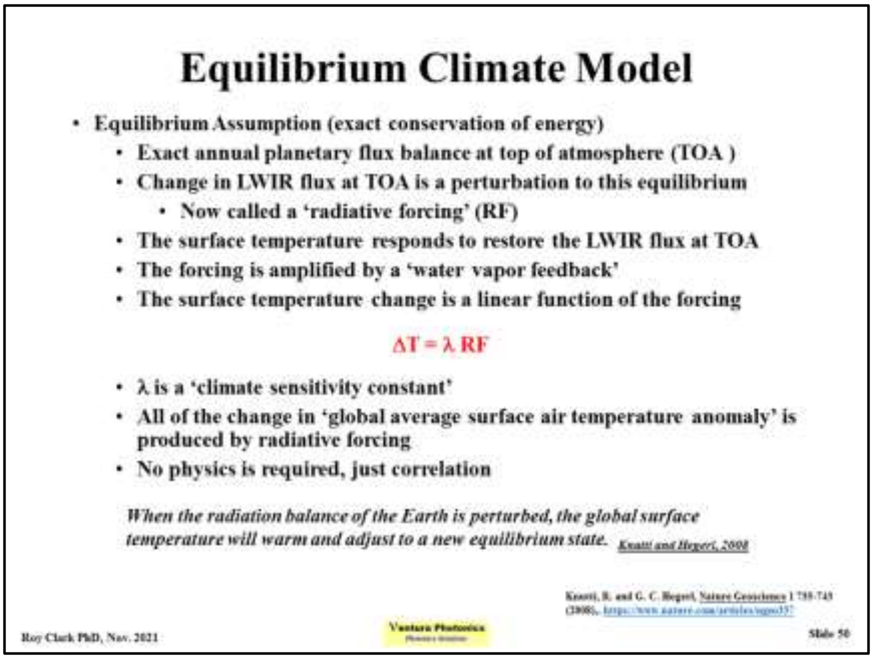

The climate models are still based on the climate equilibrium assumption. An exact annual planetary energy balance is imposed at TOA. A change in CO_2 concentration or 'radiative forcing' is considered to be a perturbation to this 'equilibrium climate state' that reduces the LWIR flux emitted at TOA. The climate system is supposed to respond with an increase in temperature that restores the flux balance at TOA.

Any increase in temperature in the climate system is also suppose to produce an increase in water vapor concentration that

The climate response to a 'radiative forcing' is also presumed to produce a linear increase in temperature and this leads to the concept of a 'climate sensitivity' to CO_2.

Natural effects such as ocean oscillations are ignored and all of the increase in temperature found in the global average temperature anomaly is presumed to have been caused by 'radiative forcing'.

No physics is required, just correlation.

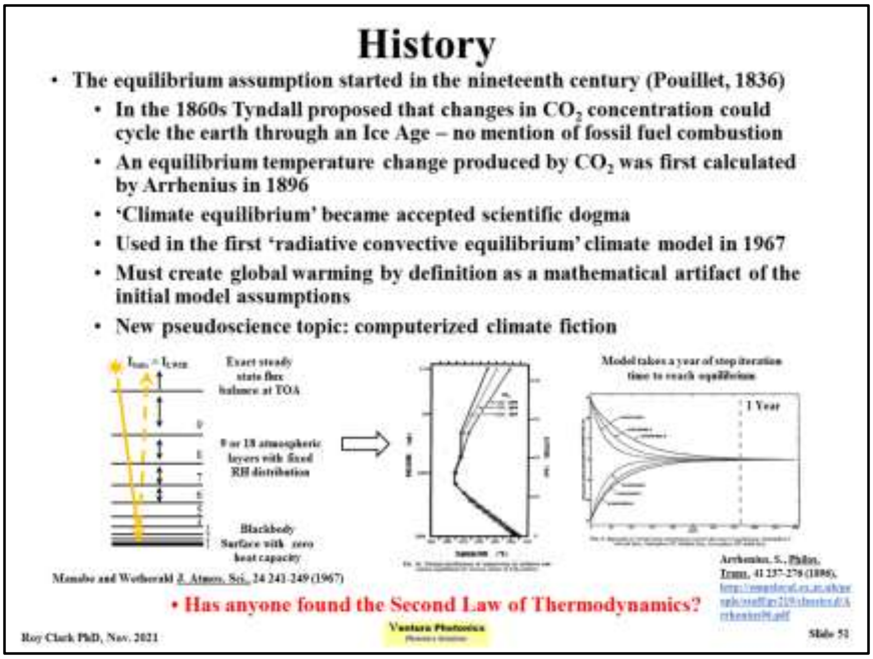

The concept of an equilibrium average climate started in the nineteenth century and has been traced back to Pouillet in 1836. In the 1860s Tyndall proposed that changes in atmospheric CO_2 concentration could cycle the earth through an Ice Age. There was no discussion of fossil fuel combustion. The first equilibrium calculations of the change in surface temperature produced by CO_2 were published by Arrhenius in 1896.

The concept of an equilibrium average climate became accepted scientific dogma and was incorporated into the first computer climate models. The first 'radiative convective equilibrium' climate model was nothing more than a mathematical platform for the development of radiative transfer and related algorithms. It created global warming by definition as a mathematical artifact of the input assumptions.

The top of the model required an exact flux balance between a 24 hour average absorbed solar flux and the upward LWIR flux. There were 9 or 18 static air layers. Each layer had a fixed value of relative humidity. This created the water vapor feedback, by definition, as a model input assumption. The surface was a blackbody surface with zero heat capacity.

Manabe has been awarded a share of the 2021 Nobel Prize for this work. The first time that this prize has been awarded for fraud.

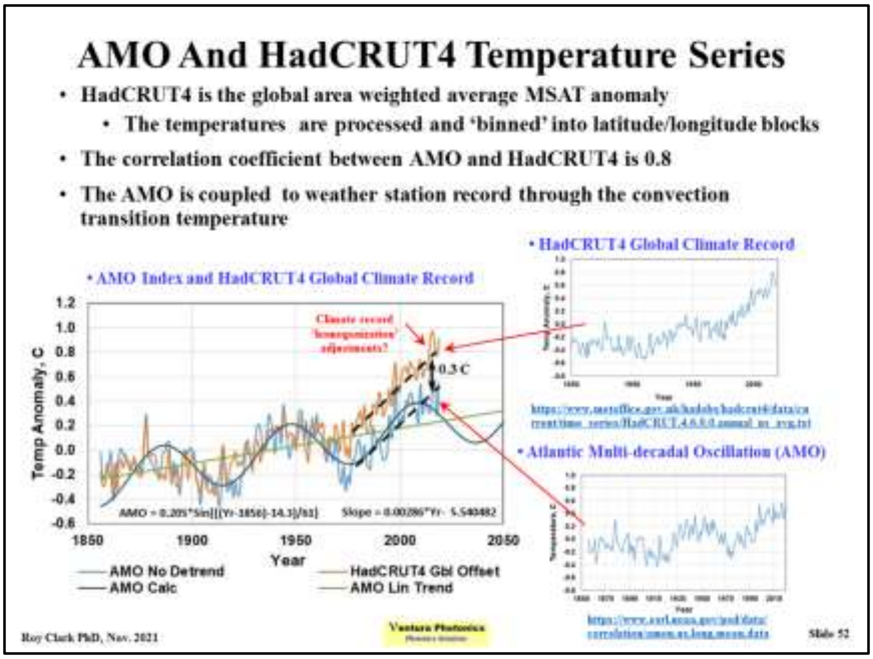

The climate model results are compared to the global average surface air temperature anomaly. This is the area weighted average weather station temperature data after it has been extensively processed ('homogenized'). The temperature anomaly is the data set with the mean removed.

The dominant term in the published temperature records such as the UK Hadley Center HadCRUT4 anomaly is the Atlantic Multi-decadal Oscillation (AMO). The correlation coefficient is 0.8.

The reason for the dominance of the AMO is the coupling of the AMO to the weather stations around the N. Atlantic basin through the convective transition temperature.

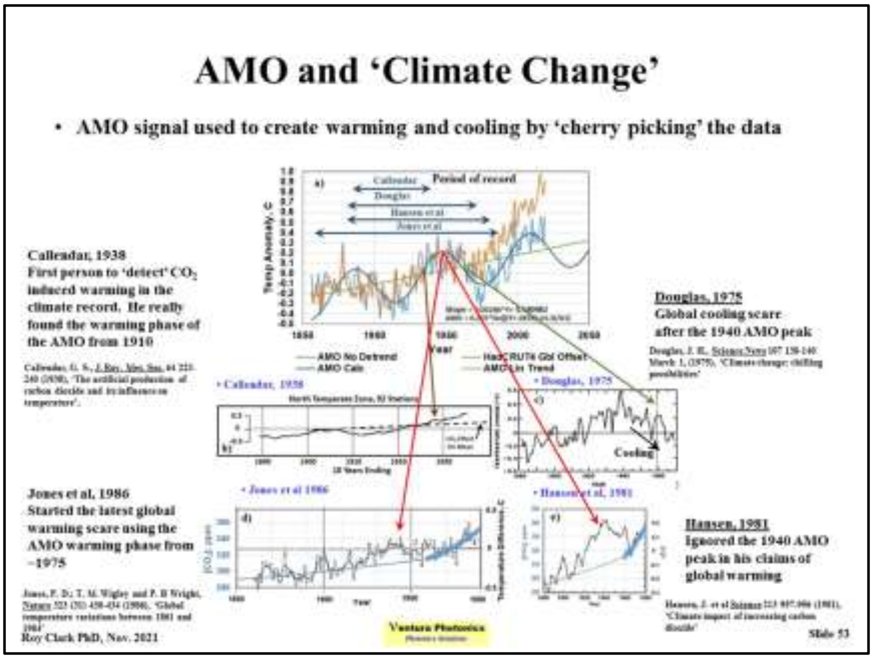

The AMO has dominated the modern climate temperature record. Climate warming and cooling have been created at different times by selecting or ignoring various parts of the temperature record ('cherry picking').

The first person to claim to have measured a CO_2 warming signal in the weather station record was Callendar in 1938. He was really measuring the AMO warming phase from 1910 to 1935.

During the 1970s there was a 'global cooling scare'. This was created using the negative phase of the AMO from 1940 to 1970.

When Hansen at al. published their paper on climate warming from CO_2 in 1981, they chose to ignore the 1940 AMO peak and call it noise. Similarly Jones et al. ignored this peak when they started to ramp up the modern global warming scare in 1986.

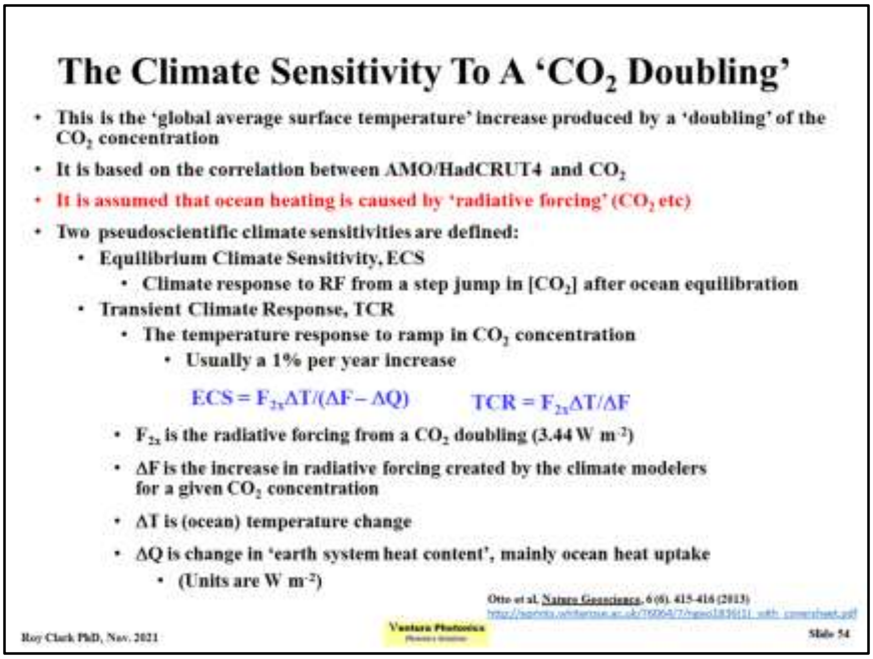

The climate modelers have not published any engineering calculations of the change in surface temperature produced by an increase in the atmospheric concentration of CO_2. Instead they have relied on the pseudoscientific concept of a climate sensitivity to CO_2. This is the hypothetical increase in global average surface temperature produced by a 'doubling' of the CO_2 concentration from 280 to 560 ppm. It is assumed that all of the increase in the HadCRUT4 temperature series has been produced by CO_2.

Two pseudoscientific climate sensitivities are defined. The first is the equilibrium climate sensitivity or ECS and the second is the transient climate sensitivity or TCS.

The ECS is the change in temperature produced by a doubling of the CO_2 concentration after the climate system has reached a new 'equilibrium state'. It is created by introducing a step increase in CO_2 concentration in a climate model and allowing the model to run to equilibrium. The step may be a doubling or a quadrupling of the CO_2 concentration.

The TCS is the change in surface temperature for a CO_2 doubling as the CO_2 concentration increases before any equilibrium is reached.

These quantities may also estimated experimentally from the assumed 'radiative forcings', the temperature response from the HadCRUT4 or similar climate record and an estimate of the earth's heating, mainly from changes in ocean heat content.

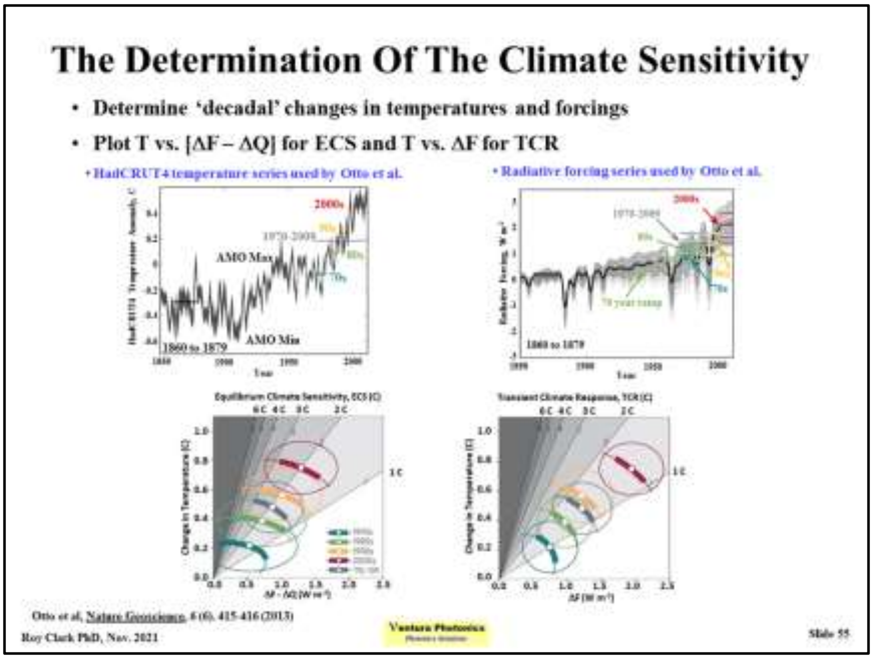

This shows estimates of the climate sensitivity published by Otto et al, 2013. They first created 'decadal' changes in temperature using the HadCRUT4 temperature series. They compared this to the radiative forcings over the same time periods estimated from the CMIP5 climate model ensemble. The ECS and TCR are determined by plotting the forcing functions vs. the temperature.

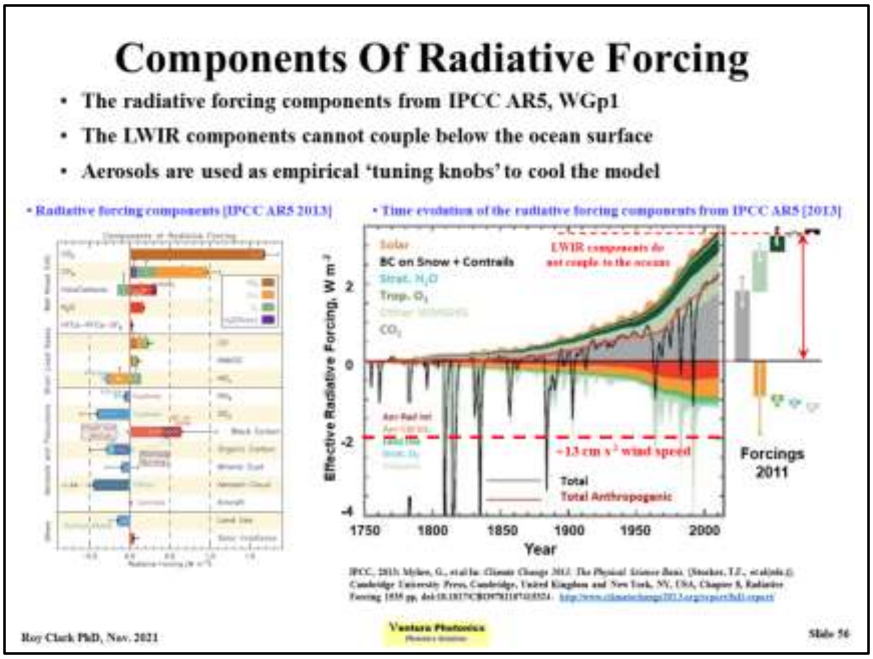

The radiative forcings used in the climate models consist of decreases in LWIR flux calculated for IR species in the atmosphere such as CO_2, CH_4 and N_2O. These changes in flux are realistic numbers that have to agree with HITRAN radiative transfer calculations. The assumptions of changes in species concentration, the 'scenarios' used in the models for economic activity are more suspect.

These LWIR forcings are combined with various 'aerosols' that are used as 'tuning knobs' to cool the models.

None of the change in LWIR flux created by the 'radiative forcings' can couple below the ocean surface and cause any ocean warming.

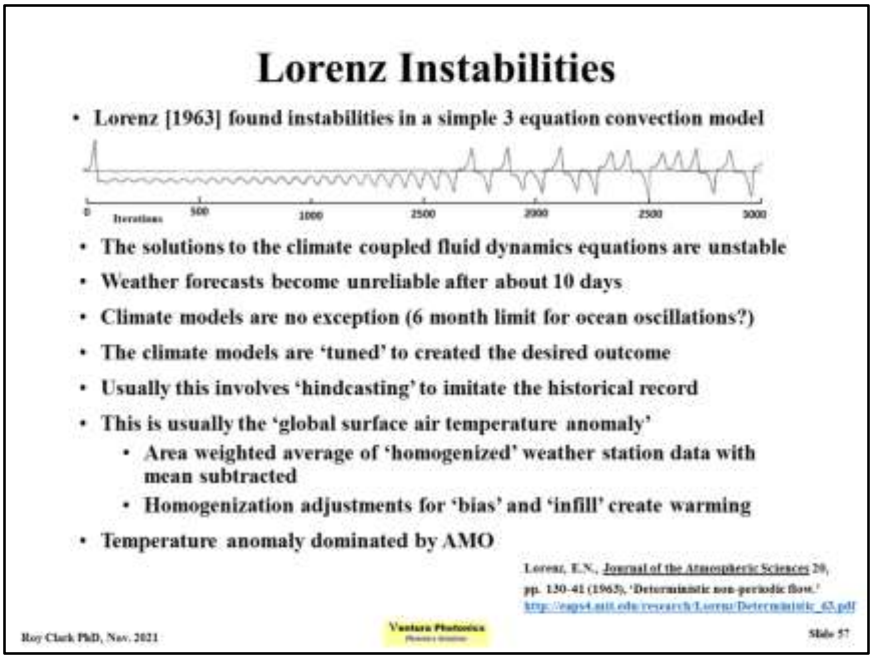

In 1963, Lorenz was working with a very simple 3 equation convection model and found that the solutions were unstable. Small changes in inputs produced large changes in the output. The rounding errors in the computer simulation accumulate and produced instabilities. The air-ocean fluid dynamics interface is also unstable and can change states. This is why the ocean oscillations are random.

Weather forecast models become unreliable after about 10 days.

The climate models are no exception. They are just modified weather forecasting models with no predictive capabilities.

The climate models are therefore 'tuned' to match the desired output. This is usually the global temperature anomaly.

The models are therefore tuned to match the AMO.

There are just an expression of the opinion of the model programmer as to what the desired result should be.

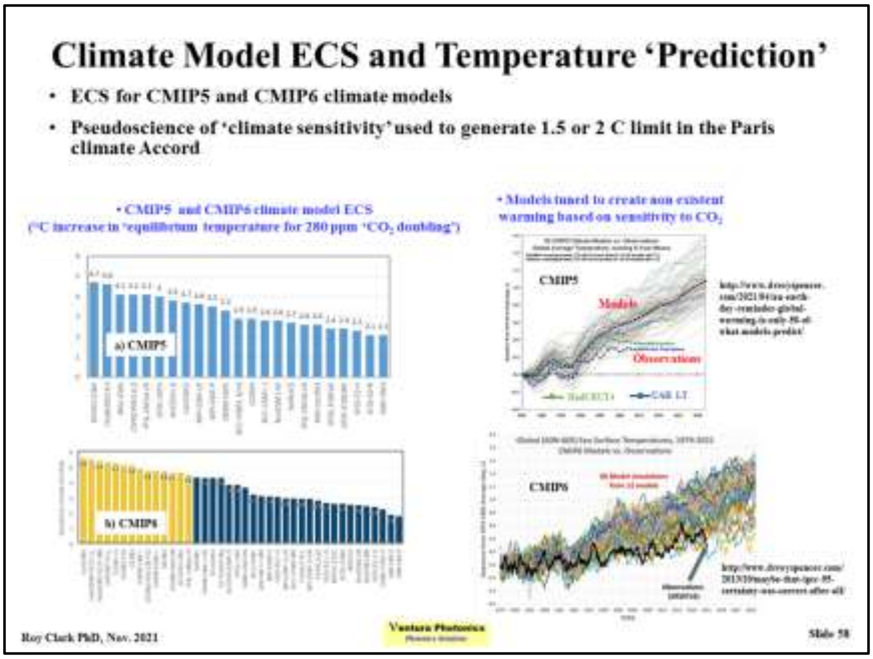

This shows the equilibrium climate sensitivities for the CMIP5 and CMIP6 climate model ensembles. The ECS should be zero.

The model results are simply noise that increases with time. This is characteristic of the Lorenz instabilities.

Future Trends?

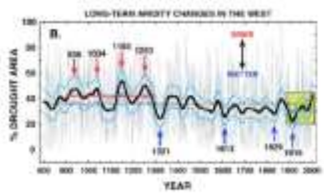

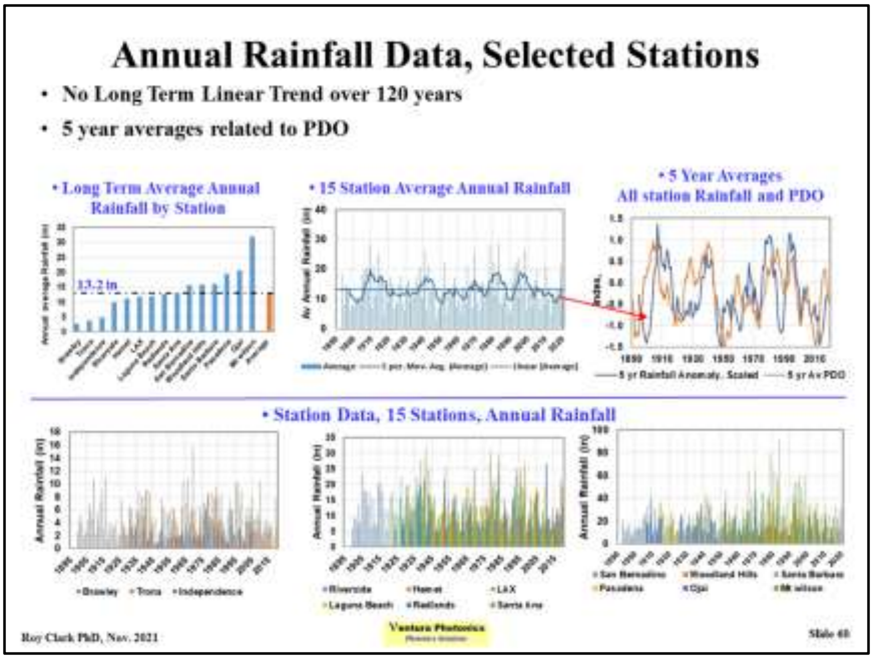

The lower plots show the annual rainfall data for 15 S. California weather stations selected for long periods of record. The upper left plot shows the long term average annual average rainfall for each station. The overall S. CA average rainfall is 13.2 inches per year.

The upper center plot shows the annual rainfall for the combined stations with a 5 year rolling average added.

The upper right plot shows the 5 year average rainfall compared to the PDO. While the two curves do not match exactly, the PDO is the main driver for the long term rainfall trends.

Over the 120 year period of record there has been no long term trend in the rainfall totals.

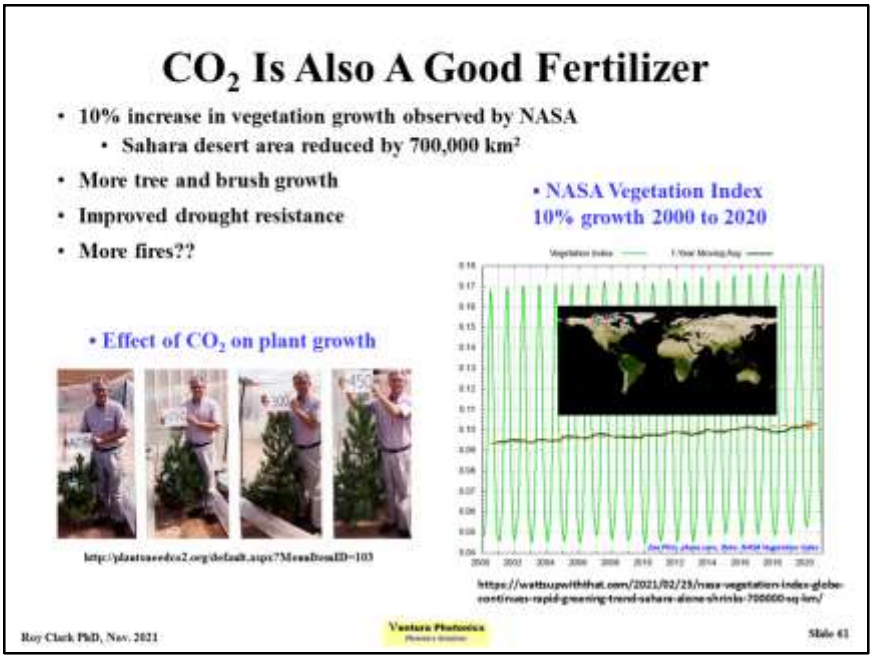

CO_2 is also a good fertilizer.

Over the last 20 years there has been a 10% increase in vegetation growth as observed by the NASA satellite vegetation index.

The Sahara desert area has been reduced by 700,000 km^2.

More CO_2 may also mean more tree and brush growth for CA fires.

The CO_2 also makes the plants more drought resistant because the leaves do not lose as much water while absorbing the CO_2.

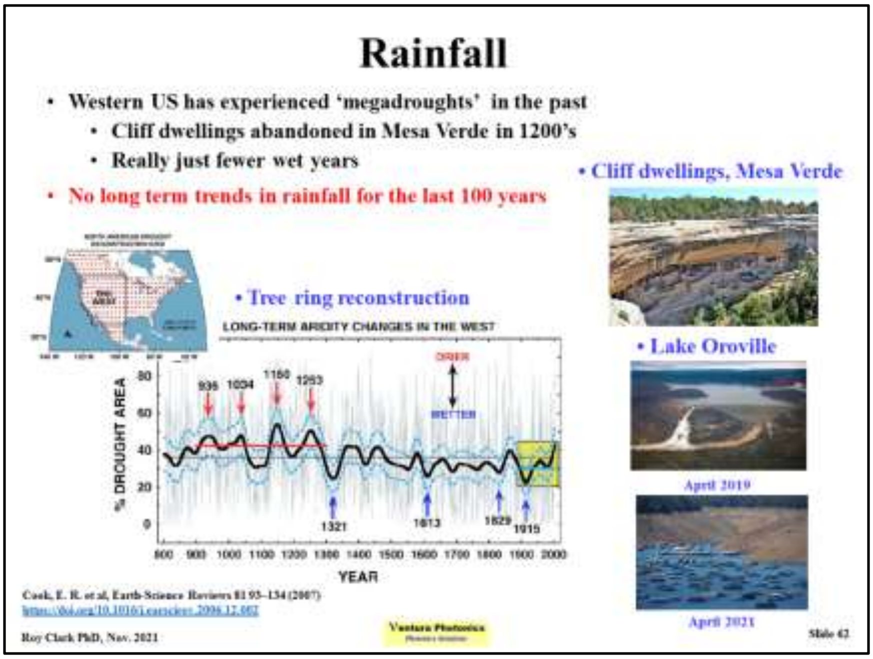

This shows a long term reconstruction of the % area of the western US impacted by drought based on tree ring analysis. There was a period of 'mega droughts' between 900 and 1300 AD probably associated with the medieval warm period. More recent data stays within the bounds of the earlier data. There is no reason to expect major changes in these long term trends.

Large short term variations in rainfall are normal – for example, Lake Oroville.

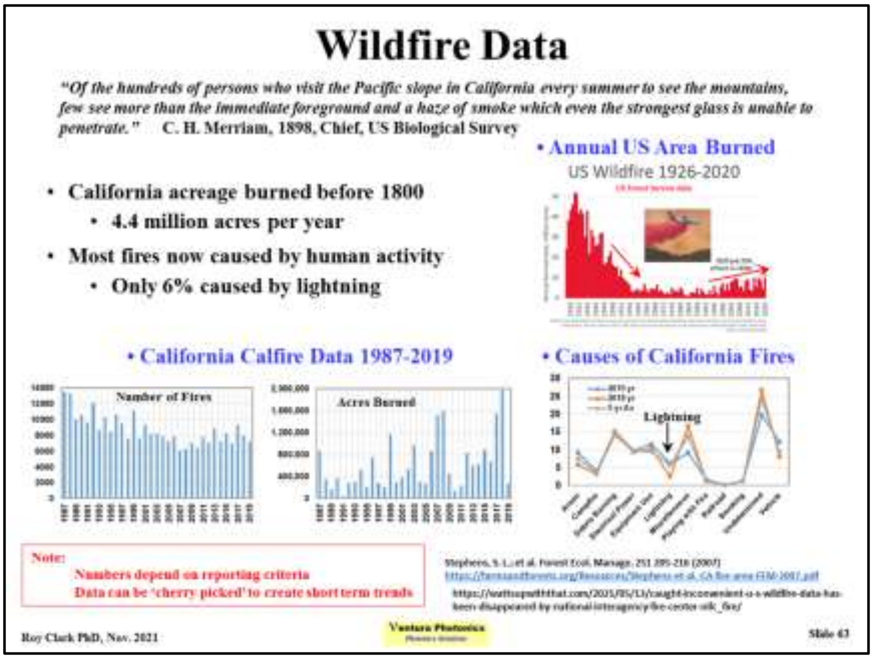

In 1898, C. H. Merriam, Chief of the US Biological Survey said that it was pointless for tourists to come and try to see the California mountain in the summer. All they would see is the smoke from the forest fires.

It has been estimated that before 1800, 4.4 million acres burned in California each year.

US acreage burned by fire has decreased since the 1920s because of more aggressive fire detection and suppression. This trend has now reversed and burned acreage is gradually increasing. The accumulated vegetation that has not burned because of fire suppression is now more vulnerable to ignition.

During the 1987 to 2019 period, Cal Fire reported that only 6% of wildfires were caused by lighting and 25% were 'unaccounted'. This mans that at least 69% of the fires were caused by human activity.

Note: The numbers used in fire reports depend on the criteria used and local records. Short term trends may not be an accurate representation of the long term record.

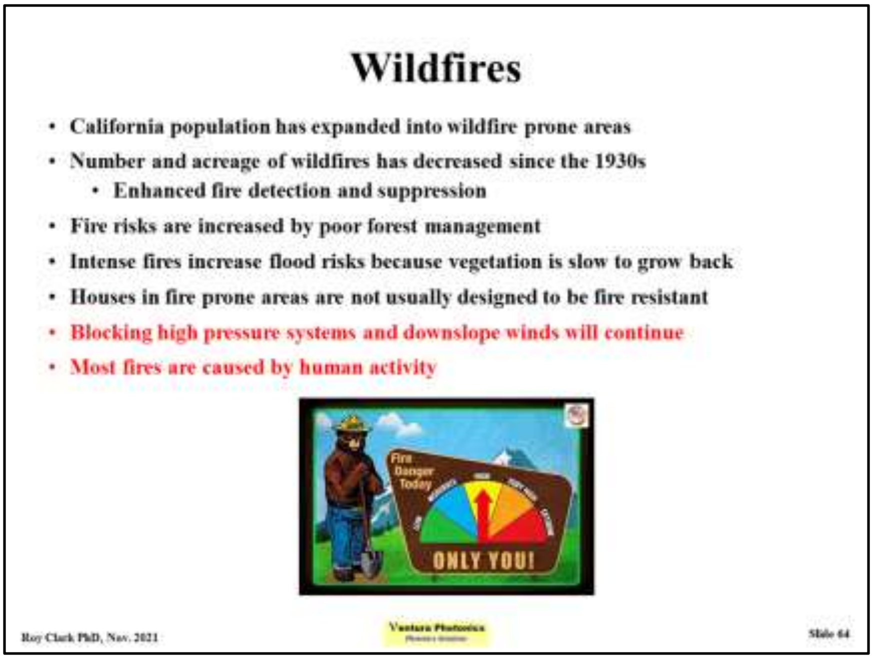

The California population has expanded into wildfire prone areas and fire risks have increased because of poor forest management and aggressive fire suppression.

Houses in fire prone areas are not usually designed to be fire resistant.

Summer fire weather with blocking high pressure systems and downslope winds will continue.

Most fires are caused by human activity.

Improved fire fuel management and better control of human related ignition sources will reduce fire ignition risks.

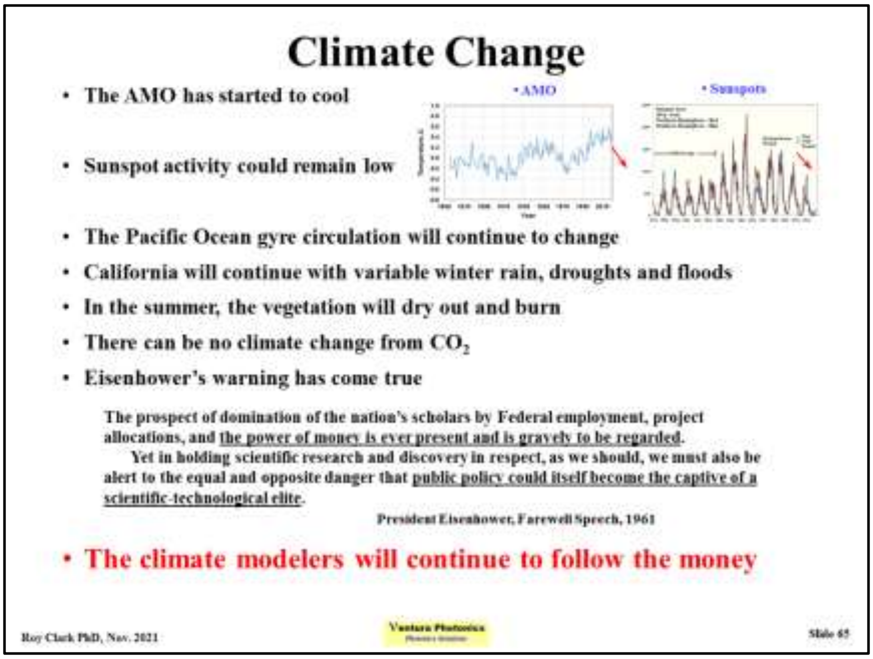

The AMO is in transition to its nominal 30 year cooling phase.

Sunspot activity has decreased, although this may change.

The Pacific Ocean gyre will continue to change and California rainfall will continue to vary.

Additional Information

- Additional information is available on my website research pages:
  www.VenturaPhotonics.com
- Climate at a Glance
  https://climateataglance.com/
- https://wattsupwiththat.com/
  (Articles, reference pages, links to other sites)